Consequences of Caspase Inhibition in Differentiating Myoblasts

Consequences of Caspase Inhibition in Differentiating Myoblasts

A dissertation presented

by

Matthew S. Owen

to

The Division of Medical Sciences

in partial fulfillment of the requirements

for the degree of

Doctor of Philosophy

in the subject of

Biological and Biomedical Sciences

Harvard University

Cambridge, Massachusetts

July 2017

Dissertation Advisor: Dr. Suzanne Gaudet Matthew S. Owen

Consequences of Caspase Inhibition in Differentiating Myoblasts

Abstract

The apoptotic caspases are proteases that mediate the process of programmed cell death. Canonically, their activation is a point of no return; however, the disruption of myoblast differentiation resulting from caspase inhibition has led some to suggest a non-apoptotic role for caspases in skeletal muscle differentiation. With no identified activation mechanism and no direct observation of cell-autonomous caspase activation in differentiating myoblasts, the validity of this model remains an open question. Here I demonstrate that there likely is no non-apoptotic role for caspases during myoblast differentiation. Rather, caspase inhibition results in the persistence of a population of cells that would have undergone apoptosis had caspases been activate, which I have dubbed UNDEAD cells for upregulators of NF-κB dependent on escape from apoptotic death. I found that this population specifically initiates NF-κB and type I interferon signaling, resulting in the secretion of inflammatory cytokines. Furthermore, I discovered that conditioned media from caspase-inhibited myoblasts is sufficient to both inhibit the differentiation of and promote the proliferation of naive myoblasts. By preventing the formation of the UNDEAD subpopulation via overexpression of Bcl-xL, I was able to prevent cytokine secretion and nearly abolish the inhibitory effects of caspase inhibition on differentiation. In sum, these results strongly contradict the established model of non-apoptotic caspase function in

myoblasts, while simultaneously establishing a novel context in which innate immune signaling can perturb the behavior of local cell populations.

Table of Contents

List of Figures

Acknowledgements

Many thank must go to those who collaborated with me on my dissertation work, especially Sebastien Vigneau and Kyomi Igarashi for their great help with single-cell RNAseq.

Thanks also to my cohort-mates in the Harvard BBS program for the wonderful friendships and for the free mental health support they provided. I am continually amazed not just at their intelligence and decency, but also at their drive to accomplish things both in their professional and personal lives.

Thank you to my first Dissertation Advisory Committee – Anthony Letai, Galit Lahav, and Gary Yellen – for their encouragement, guidance, and patience with an overly risky project. Thanks too to my second committee – Nika Danial, Constance Cepko, and Andrew Lassar – for their helpful feedback.

Thank you to members of the Gaudet lab, past and present: Robin Lee, Kate Savery, Xianfang (Donna) Xia, Amir Aref, Mohammad Qasaimeh, Colin Waters, Martin Reindl, Constanze Kainz, Chris Mukasa, Michelle Lin, Nichole Jones, Shibin Mathew, Ruth Brignall, and Amy Thurber for sharing their knowledge and making the lab such a wonderful environment in which to work. Special thanks must go to Robin and Kate for helping me get started in the lab.

A great many thanks must go to my thesis advisor, Suzanne Gaudet, for her support and mentorship. Suzanne's optimism and enthusiasm has always been a crucial counterpoint to my more skeptical and pessimistic outlook. She has also set a wonderful example of maintaining a good work-life balance.

Thanks to my parents, Stephen and Patricia Owen, for not just loving and providing for me, but also for nurturing my curiosity and setting a wonderful example of how to approach the world in a thoughtful manner. My debt to them is one that can never be repaid. Thanks also to my brother, Jeffrey Owen, for serving as a role model for high scholastic achievement.

I also must thank my parents-in-law, Anthony and Rauchelle Smiraglia, for welcoming me into their family and being nothing but supportive.

Most of all, I would like to thank my best friend and wife, Christina Smiraglia, for her incredible support, both personal and professional, during the entirety of our relationship. Even at the lowest points in my research, I could always look forward to coming home to her (and our cat Starkey). I have no doubt that our love for each other was essential to my ability to complete my dissertation research.

Chapter 1: Introduction

Most biological organisms are in a constant state of cellular flux, maintaining a balance between cell birth and cell death. It is estimated that up to 70 billion cells die each day in an average human adult (Pelengaris and Khan, 2013), making cell death pathways extremely important for maintenance of homeostasis. Cells can be triggered to die for a variety of reasons, including cellular damage, metabolic stress, direct killing by immune cells in cases of infection or potential tumorigenesis, or simply because of natural turnover within a given tissue. However, it is important not just *that* a given cell dies, but also *how* it dies. Although cells occasionally die in an uncontrolled fashion, most cell death *in vivo* is the result of a programmed cell death pathway of some sort. Various kinds of programmed necrosis have been documented, but the best characterized cell death pathway is apoptosis. An essential difference between apoptosis and the other death pathways is that apoptosis is immunologically silent, allowing cells to die without triggering inflammation. An apoptotic cell is broken down in an orderly fashion: protein synthesis is halted, genomic DNA is degraded, and signals are engaged that mark the remains of the cell for prompt engulfment by phagocytic immune cells.

The systematic breakdown of cells during apoptosis is orchestrated by members of the caspase family of cysteine proteases, which are distinct from other proteases in having a strong preference for cleaving after aspartic acid residues. Mammalian caspase family members can be broken into 3 major groups: inflammatory (caspases-1, 4, 5, 11, and 12), which are best known for processing interleukin 1; effectors (caspases-3, 6, and 7), which cleave substrates that carry out the destruction of the cell; and initiators (caspases-2, 8, 9,

and 10), which cleave and activate the effectors in response to internal and external signals (Taylor et al., 2008). The external signals come in the form of death ligands of the tumor necrosis factor (TNF) family, which trigger the extrinsic apoptosis pathway by activating caspases-8 and 10 in protein complexes associated with death receptors (Walczak, 2013).

Cells infected with a pathogen can be induced to undergo apoptosis to prevent their use in enabling the pathogen's replication. Unsurprisingly, some pathogens try to prevent this by inhibiting caspase activation. Viral caspase inhibitors thus far identified include CrmA from cowpox, P35 and P49 from baculovirus (Callus and Vaux, 2007), and F1L from vaccinia (Zhai et al., 2010). Recently, the first bacterial caspase inhibitor, NleF, was identified in pathogenic E. coli (Blasche et al., 2013). It has been observed that caspase inhibition in the context of TNF treatment can lead to necroptosis, an inflammatory form of programmed cell death (Degterev et al., 2005). This response may be an adaptation to strengthen the immune response in areas where pathogens are resisting removal via the default cell death pathway. As part of this dissertation, I detail another signaling pathway, discovered in the context of myoblast differentiation, that may also function to increase inflammation when caspase inhibition is preventing apoptosis.

1.1 The Intrinsic Apoptosis Pathway

In the absence of signals from death receptors, initiation of apoptosis must go through the intrinsic apoptosis pathway, sometimes referred to as the mitochondrial

apoptosis pathway (Fig 1.1). Activation via this pathway hinges on one specific event, namely the release of factors from essentially all of a cell's mitochondria in a process called mitochondrial out membrane permeabilization (MOMP). During MOMP, pores form in the outer mitochondrial membrane, allowing the release of proteins and other molecules that reside in the mitochondrial intermembrane space. The most important molecule released is cytochrome c, a component of the electron transport chain. Upon entry to the cytoplasm, cytochrome c interacts with apoptosis protease activating factor 1 (Apaf-1) and ATP to form a heptameric holoenzyme called the apoptosome that can recruit and activate caspase-9 (Hengartner, 2000). Active caspase-9 can then go on to activate the effector caspases, except that both caspase-9 and the effector caspases are actively inhibited by X-linked inhibitor of apoptosis protein (XIAP). However, another factor released from the mitochondria during MOMP, direct IAP binding protein with low pI (DIABLO, a mouse homologue of the human protein SMAC) directly inhibits XIAP, thus releasing the brake on caspase activation. The result is a rapid, switch-like activation of caspases following MOMP, making MOMP a *de facto* point of no return in terms of cell death (Tait and Green, 2013).

MOMP is regulated via complex interactions between members of the B-cell lymphoma 2 (Bcl-2) family. Family members Bcl-2-associated X protein (Bax) and Bcl-2 homologous antagonist/killer (Bak) can both permeabilize the outer mitochondrial membrane by oligomerizing and forming pores (Cosentino and García-Sáez, 2017). This process is facilitated by the so-called BH3-only proteins, pro-apoptotic members of the Bcl-2 family. The anti-apoptotic Bcl-2 proteins include Bcl-2 itself, B-cell lymphoma-extra large (Bcl-xL), and myeloid cell leukemia 1 (Mcl-1). These proteins inhibit MOMP in two ways:

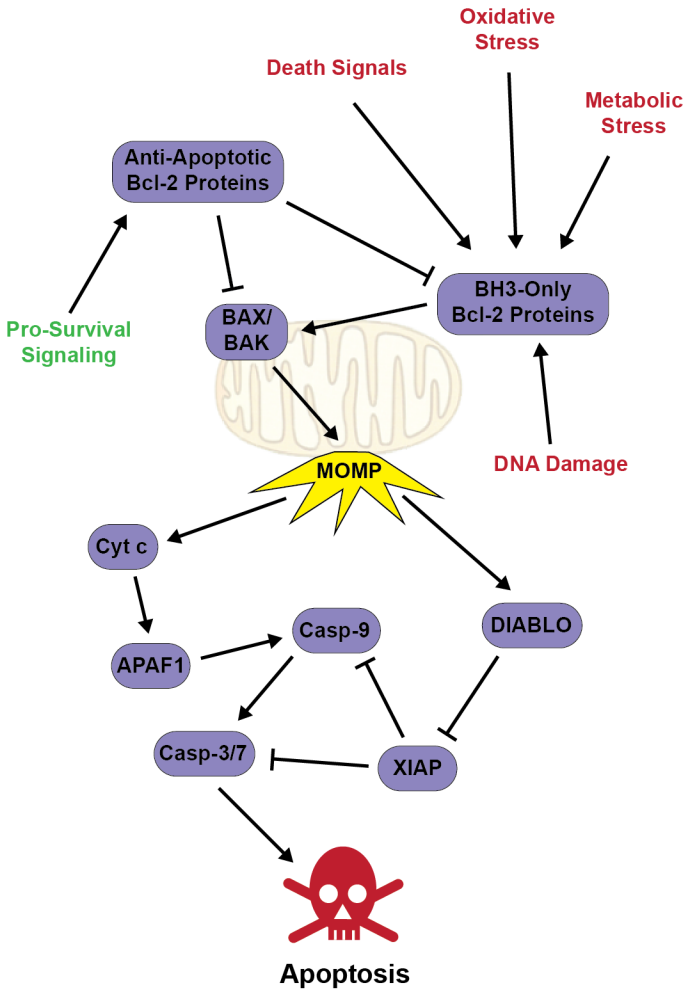

Figure 1.1: The Intrinsic Apoptosis Pathway The intrinsic pathway of apoptosis is activated when accumulation of cellular stresses signal through members of the Bcl-2 family of proteins to induce mitochondrial outer membrane permeabilization (MOMP). Activation of MOMP results in the exit of cytochrome c and DIABLO from the mitochondrial intermembrane space. Cytochrome c interacts with APAF1 to activate caspase-9, which in turn cleaves and activates the effector caspases. DIABLO antagonizes the endogenous caspase inhibitor XIAP to release the brake on full caspase activation, resulting in rapid cellular disassembly.

1) binding to Bax and Bak and preventing them from oligomerizing, and 2) binding to BH3-only proteins, keeping them away from Bax and Bak (Kroemer et al., 2007). The various BH3-only proteins can be upregulated or activated in response to a variety of different signals including metabolic stress, growth factor deprivation, DNA damage, and signals from death receptors (the extrinsic apoptosis pathway generally activates MOMP, even in situations where it is not necessary to achieve cell death). For example, BH3 interacting-domain death agonist (Bid) is cleaved and activated by initiator caspases responding to signals from death receptors (Li et al., 1998a) while p53 upregulated modulator of apoptosis (Puma) is transcriptionally controlled and can be upregulated by the tumor suppressor p53 (Nakano and Vousden, 2001) in response to DNA damage, as well as in other contexts. Generally, when the concentration of the BH3-only proteins relative to the anti-apoptotic proteins becomes high enough, MOMP will be initiated. However, in practice, this signal integration is more complex, due in part to the variable binding affinities between different Bcl-2 family members (DeBartolo et al., 2012). Nevertheless, overexpression of anti-apoptotic Bcl-2 proteins usually results in cells that are able to resist apoptosis, even in the face of substantial cellular stress (Yip and Reed, 2008).

1.2 Non-Apoptotic Roles for Apoptotic Caspases?

The classification of caspases as either apoptotic or inflammatory was done very early in the study of mammalian caspases, and further study has shown that grey areas exist

between the two categories. Caspases can have very narrow substrate specificity compared with other proteases, making them excellent candidates for signal propagation. The sheer number of caspases in mammals (10 in mice, 11 in humans) compared with the number in nematodes (4) implies that alternate, adaptive roles have been found for additional family members. In the case of the Bcl-2 family of proteins, it has become increasingly appreciated that certain family members function in roles beyond just regulating MOMP. For example, Bcl-2 death promoter (Bad) has been shown to complex with glucokinase and aid in the regulation of glucose metabolism (Danial et al., 2003). Perhaps caspases could be similarly fulfilling other roles outside of the context of apoptosis.

There is strong evidence that caspase-8 does have roles other than initiating apoptotic signaling. These roles may include: T-cell activation, inflammasome regulation, and regulation of a programmed necrosis pathway (Feltham et al., 2017; Salmena et al., 2003). Caspase-8 may be somewhat unique in being able to serve additional functions, as it is activated as part of large protein complexes. Varying the composition of the complex can alter the substrates of the enzyme and thus the signal that is propagated (Guicciardi and Gores, 2009). In contrast, caspase-3, while potentially recruited to the apoptosome for activation by caspase-9 (Hill et al., 2004; Yuan et al., 2011), is not generally thought to interact with its substrates as part of a complex. On the other hand, the consequences of limited caspase-3 substrate cleavage can be severely detrimental, as seen in the cases of isolated MOMP of a few mitochondria (Ichim et al., 2015) and depletion of XIAP in MOMP-incompetent cells treated with a death ligand that triggers a caspase-8-mediated caspase-3 activation (Albeck et al., 2008). In both cases, sub-lethal caspase-3 activity led to extensive

DNA damage following activation of caspase-activated DNAse (CAD). These examples suggest that non-apoptotic activation of caspase-3 would need to severely limit cleavage of many canonical apoptotic substrates in order to avoid serious adverse consequences for the cell.

Despite the seeming difficulties involved, caspases involved in intrinsic apoptosis have been proposed to function in a non-apoptotic capacity in a variety of differentiation pathways. In two such instances potential DNA damage would not be a concern, as caspases were suggested to regulate the enucleation of lens cells (Ishizaki et al., 1998; Wride et al., 1999) and of erythrocytes (Carlile et al., 2004; Zermati et al., 2001). In the case of lens cells, a caspase-6-like activity was measured in lysates from differentiating lens cells, and caspase inhibition disrupted the process (Foley et al., 2004); however, a later study found that lens cells from caspase-3/caspase-6 double knockout mice continued to show caspase-like activity and differentiated normally (Zandy et al., 2005), suggesting that there was likely another source of this proteolytic activity. In the case of erythrocyte differentiation, knockdown of caspase-3 was found to result in a reduction of enucleated cells; however, it was also discovered that both caspase-3 knockdown and chemical caspase inhibition resulted in the arrest of many erythroid progenitors at the pronormoblast stage, well before the onset of enucleation (Carlile et al., 2004), and that signs of caspase substrate cleavage were absent during the enucleation process (Krauss et al., 2005). Thus, the theory that non-apoptotic caspase activation governs “partial apoptosis,” while initially appealing, is likely invalid.

Apoptotic caspases have also been proposed to participate in differentiation processes that bear no resemblance to apoptosis. Caspase inhibitor treatment and Bcl-2 overexpression were observed to inhibit the differentiation of U937 cells into macrophages following treatment of 12-O-tetradecanoylphorbol 13-acetate (TPA) (Sordet et al., 2002). In megakaryocytes, cleaved caspase-3 was detected by antibody staining in cytoplasmic regions around where proplatelets form, and proplatelet production was hindered by Bcl-2 overexpression and caspase inhibitor treatment (De Botton et al., 2002). Caspase-3 deficiency in embryonic stem cells (ESCs) caused them to differentiate less efficiently in response to retinoic acid, while expression of a constitutively active form of caspase-3 potentiated this differentiation process (Fujita et al., 2008). It was suggested that caspase cleavage of the pluripotency maintaining transcription factor Nanog promotes differentiation of the ESCs. Similarly, it was reported that caspase cleavage of the transcription factor Pax7 promoted the differentiation of satellite cells into myoblasts (Dick et al., 2015). Notably, none of these reports details any mechanism for how caspases are being activated beyond the idea, in a few of them, that MOMP is involved in some way. Also, other than the aforementioned cleavage of Nanog and Pax7, no mechanisms are put forth for how caspases are mediating the differentiation process. Most importantly, in none of these cases is a mechanism proposed for how a cell can activate apoptotic mediators without then triggering apoptosis.

The current state of this field leaves many questions unanswered: are caspases associated with intrinsic apoptosis truly activated in the context of differentiation? If so, how do cells avoid apoptosis? And, if there is no non-apoptotic caspase activation, why

does caspase inhibition affect differentiation? In my dissertation research, I have addressed these questions using skeletal muscle differentiation as a model. In Chapter 2, I present evidence that there is no non-apoptotic caspase activation in skeletal muscle differentiation, but that, instead, caspase inhibition leads to the formation of a novel sub-population of cells that are able to survive, despite undergoing MOMP, and are also able to antagonize the differentiation of neighboring myoblasts. I also show that this sub-population specifically activates innate immune signaling pathways, resulting in the secretion of inflammatory cytokines. Finally, in Chapter 3, I discuss the implications of my findings to the field of non-apoptotic caspase function. I also discuss how inflammatory signaling coming from caspase-inhibited cells may affect the course of diseases like cancer and how this may affect treatment option

Chapter 2: Results

Contributions

I planned and carried out most the experiments for this project, but I must acknowledge the essential work of my collaborators. Kyomi Igarashi and Sébastien Vigneau of the Gimelbrant lab at Dana Farber Cancer Institute ran the inDrop cell sorting device on samples I prepared. Kyomi also prepped the RNAseq library for sequencing and Sébastien assisted with processing the raw RNAseq data. Alexander Gimelbrant and Suzanne Gaudet assisted with the clustering analysis and gene set enrichment analysis. The mouse cytokine array data samples that I prepared were run by Willa Zhou and Raven Vlahos, and analyzed by Willa, Raven, and Michaela Bowden.

2.1 Introduction

Although non-apoptotic caspase activation has been proposed in a wide variety of differentiation processes, one of the most heavily studied is skeletal muscle differentiation, also referred to as myogenesis. Specifically, studies have focused on myogenesis in adults, where it works to regenerate damaged muscle tissue. In adults, a population of muscle stem cells, termed satellite cells, resides within muscle tissue in a quiescent state (Gamble et al., 1978). When muscle is damaged, nearby satellite cells begin asymmetric division, generating a population of muscle precursor cells called myoblasts. Myoblasts continue to proliferate until they are numerous enough to repair the local damage, at which point they drop out of the cell cycle and start to differentiate. The myoblasts elongate as they

transition into myocytes, which then begin fusing to each other, forming increasingly large, multi-nucleated myotubes (Bischoff and Holtzer, 1969). These myotubes can self-organize into *de novo* muscle fibers or fuse to existing fibers.

Myogenesis is primarily governed by a family of helix-loop-helix transcription factors called the myogenic regulatory factors. Of these, MyoD and myogenic factor 5 (myf5) are present in myoblasts at baseline. In contrast, myogenin is not expressed until later in the differentiation program, when, in more mature myoblasts and in myocytes, it aids in activating the expression of skeletal muscle-specific genes like those that code for the specific forms of actin and myosin found in mature muscle fibers (Molkentin and Olson, 1996).

Myogenesis can be modeled *in vitro* using tissue culture cell lines. Most prominent among these models is the mouse myoblast cell line C2C12. C2C12 cells were originally derived from dystrophic mouse thigh muscle (Yaffe and Saxel, 1977) and can be induced to differentiate by switching them to low serum differentiation media, typically with 2% horse serum. The low serum environment leads to exit from the cell cycle, which triggers the differentiation program. Differentiation can be functionally evaluated by measuring the efficiency of myoblast fusion using a metric called the fusion index, a measure of the percentage of total nuclei that are found in multi-nucleated myotubes (Fig 2.3B).

Reports claiming a role for caspases in myogenesis began with the observation that caspase-3 knockout mice have abnormally small muscles (Fernando et al., 2002). Primary myoblasts derived from these mice were unable to differentiate efficiently *in vitro* and were somewhat abnormal in markers of progression through myogenesis (Fernando et al., 2002).

Measurements of caspase activity in lysates of C2C12 cells induced to differentiate found a peak in caspase activity 24 hrs after serum withdrawal (Fernando et al., 2002). Use of an activity-based probe (biotinylated covalent caspase inhibitor) showed that caspase-9 was activated during the early course of differentiation (Murray et al., 2008). Treatment of C2C12s with both pan-caspase (Murray et al., 2008) and purportedly caspase-3 directed (although I would note that this inhibitor would substantially inhibit other caspases) inhibitors (Fernando et al., 2002) resulted in substantial decreases in the fusion index at numerous timepoints following serum withdrawal. A similar effect was observed in shRNA-mediated knockdown of caspase-9 (Murray et al., 2008). Taken together, these results certainly indicate that the intrinsic apoptosis pathway is activated in differentiating myoblasts and that its inhibition can hinder differentiation.

In addition to proposing a general need for caspase activation in myoblast differentiation, researchers posited that a pair of caspase substrates were playing a role in mediating the differentiation process. The first was mammalian sterile 20-like kinase-1 (MST1). Researchers found that expressing a truncated form of the protein, mimicking a caspase cleavage, was able to rescue the differentiation of caspase-3 knockout myoblasts, although expressing the same fragment in wild-type (WT) myoblasts lead to widespread cell death after several days (Fernando et al., 2002). The other substrate was inhibitor of caspase-activated DNAse (ICAD), which, when cleaved by caspases, loses its ability to inhibit the activation of caspase-activated DNAse (CAD) (Larsen et al., 2010). In this last study, the researchers demonstrated that both knockdown of CAD and expression of an uncleavable form of ICAD resulted in a decrease in myoblast fusion, arguing that CAD activation is a

necessary part of myoblast differentiation (Larsen et al., 2010). Specifically, they hypothesized that the drastic epigenetic changes needed for differentiation are enabled by CAD-mediated DNA double strand breaks. However, because of the limited supporting evidence and lack of characterization of the role for DNA damage in directing specific epigenetic changes, this explanation seems tenuous. Moreover, when considering functions for both MST1 and CAD in myogenesis, the case for one substrate would also seem to undermine the other. Indeed, the MST1 rescue experiment shows that CAD activation is not necessary for efficient differentiation (Fernando et al., 2002), and the negative effects from loss of CAD activation show that MST1 activation is not sufficient for it (Larsen et al., 2010). Add to this that both ICAD and MST1 are substrates of caspase-3 during apoptosis, and it becomes apparent that a strong explanation is lacking for how caspase activation plays a role in myogenesis.

In addition to the lack of a solid mechanism explaining the downstream consequences of caspase activation in differentiating myoblasts, there is also not much evidence for how the implicated caspases could be activated. One study suggests that MOMP could be the trigger, given the apparent activation of caspase-9 and the inhibition of differentiation seen with overexpression of, presumably MOMP inhibiting, Bcl-xL (Murray et al., 2008). However, their own data show no signs of mitochondrial permeabilization in differentiating myoblasts (Murray et al., 2008), and they provide no explanation for how MOMP could occur without activating apoptosis. The existence of these limitations does not necessarily indicate that the conclusions of the previous studies are incorrect, but stronger observations will be required to confidently conclude anything.

A limitation that is shared by all of the reports concerning the role of caspases in myogenesis is their use of population-based assays at fixed time points. While this approach is fairly standard, it has especially large caveats in this case, because a measurement that averages over the entire population of cells will be unable to distinguish between caspase activation in differentiating and apoptotic cells. Truly demonstrating a non-apoptotic caspase activation would require identifying caspase activation at the level of individual cells and then establishing that the fate of that cell is not apoptosis. As part of the work of my Ph.D. thesis, I undertook this using a fluorescent-protein-based biosensor to measure caspase activity in live cells and determine whether they were activated in differentiating myoblasts.

2.2 Caspase activation during myogenesis is detectable only in apoptotic cells

The claims that caspases play a non-apoptotic role in skeletal muscle differentiation thus far lack strong evidence. So, to address the question of whether caspases are activated in differentiating myoblasts, I set out to monitor the differentiation process in real time, using a live-cell caspase activity reporter. Fluorescent-protein-based biosensors have been used for many years to measure a variety of indices, including gene expression level, protein localization, organelle pH, and metabolite concentration (Hung et al., 2011; Johnson et al., 2009; Li et al., 1998b). One of the earliest sensors, in fact, was designed to measure caspase activity. It was based around Förster resonance energy transfer (FRET) between a blue

fluorescent protein (BFP) and a green fluorescent protein (GFP) connected by a peptide linker containing a caspase cleavage site (Xu et al., 1998). Upon caspase activation, the linker would be cleaved, separating the two fluorescent proteins beyond the maximal radius over which FRET can occur. This effectively "de-quenches" the BFP, and the resulting increase in its fluorescence can be measured dynamically as an indicator of caspase activity.

I began my efforts at detecting real-time caspase activation with a FRET-based reporter obtained from the lab of Peter Sorger, which used cyan fluorescent protein (CFP) and yellow fluorescent protein (YFP) (Albeck et al., 2008). However, it quickly became apparent that expressing and exciting multiple fluorescent proteins was too toxic for the myoblasts, necessitating a change in strategy. I acquired a different fluorescent caspase reporter (NES-mVenus; (Beaudouin et al., 2013)), which consists of a yellow fluorescent protein (mVenus) connected to a nuclear export signal (NES) via a peptide linker containing a strong caspase cleavage site (Fig 2.1A). Under basal conditions, the steady state concentration of mVenus in the nucleus is very low, but upon caspase activation and subsequent removal of the NES, there is an increase in nuclear fluorescence corresponding to the integrated caspase activity over time. This integration over time makes the reporter very sensitive at the cost of temporal resolution; however, because I did not know the duration or intensity of caspase activation in each individual myoblast, I endeavored to make the reporter as sensitive as possible. Therefore, I modified the amino acid in the linker immediately c-terminal to the cleavage site (the P1' residue), changing it from an arginine to a glycine. Previous work has demonstrated that an arginine in that position greatly increases the specificity of a caspase reporter for the executioner caspases over the

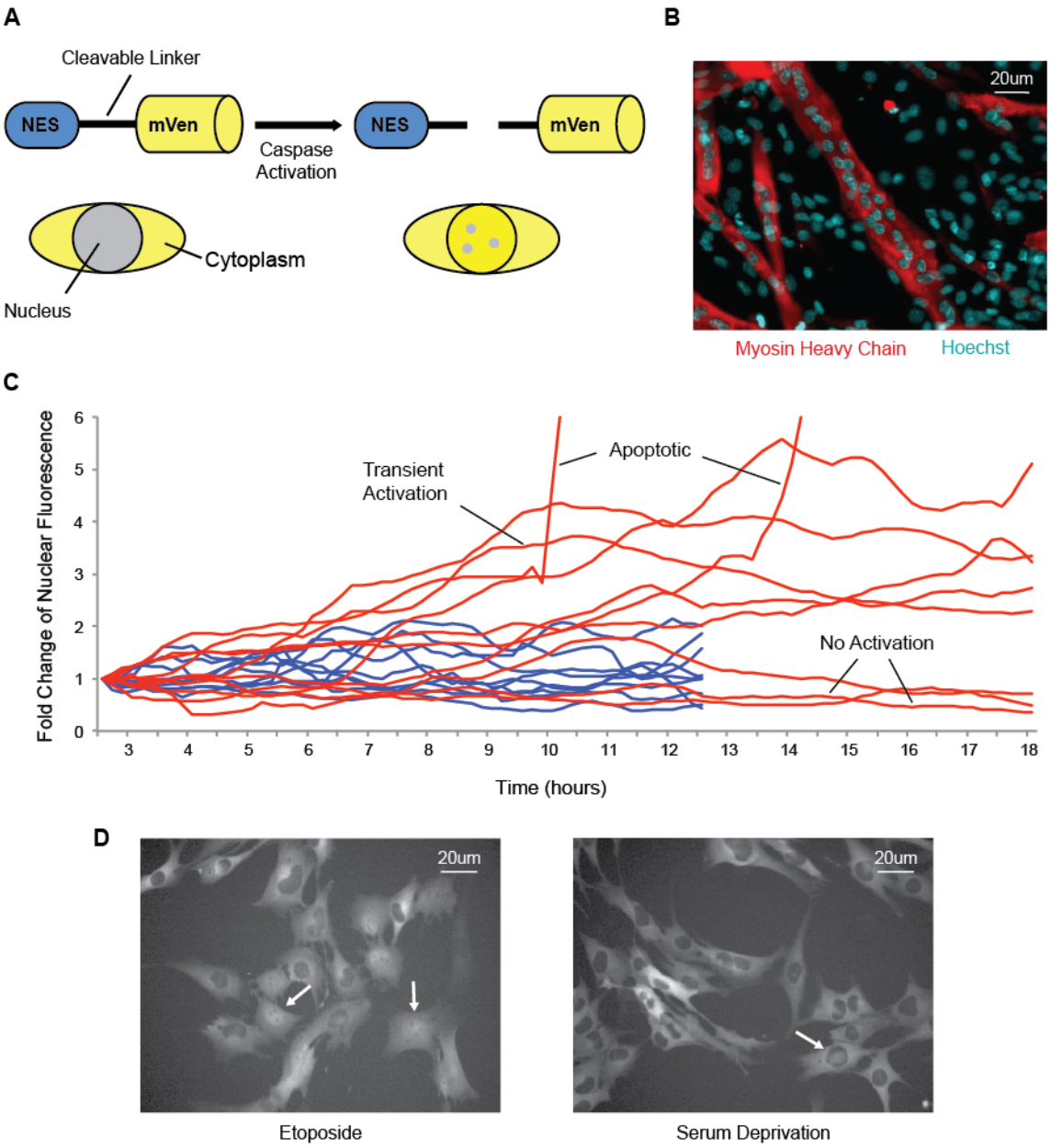

Figure 2.1: Non-apoptotic caspase activation is not detected in differentiating myoblasts by a live-cell caspase reporter A) Diagram of live-cell caspase activity reporter. Caspase activation leads to removal of the nuclear export signal (NES) from mVenus, allowing it to enter the nucleus. Nuclear fluorescence integrates signal over an extended period of time. B) C2C12 cells stably expressing NES-DEVDG-mVenus and mCherry-NLS were differentiated by serum deprivation for 5 days then stained for myosin heavy chain (red) or Hoechst (cyan). Large, multi-nucleated myotubes demonstrate that the cell line can differentiate efficiently. C) Single cell traces of relative nuclear fluorescence from C2C12 cells treated with etoposide (red) or induced to differentiate by serum deprivation (blue; imaging begins 24 hrs after induction). Etoposide-treated cells display a range of activation dynamics, while traces from differentiating cells lack clear evidence of caspase activation. Representative Traces from 2 independent experimentsD) C2C12s imaged for mVenus following treatment with 125uM etoposide (left) or while differentiating (right). Arrows in the image on the left demonstrate clear evidence of caspase activation, with a distinct nuclear morphology. Cells in pictured on the right lack this morphology but occasionally see non-specific nuclear fluorescence from neighboring cells or out of focus cytoplasm (arrow).

initiators, but at the cost of sensitivity (Albeck et al., 2008; Stennicke et al., 2000). Thus, placing a highly-permissive glycine in that position should maximize sensitivity to whichever caspases are activated during myogenesis.

I generated a C2C12 cell line stably expressing NES-mVenus and mCherry-NLS (an RFP variant fused to a nuclear localization signal, used to demarcate the nucleus for segmentation and tracking) and used fluorescence activated cell sorting (FACS) to generate a mixed population of cells that expressed both reporters at a high level. I confirmed that these cells were able to differentiate upon serum deprivation (Fig 2.1B) and then tested the efficacy of the caspase reporter by treating the cells with the DNA damaging agent etoposide, followed by time-lapse live-cell imaging. Etoposide treatment resulted in substantial nuclear localization of the mVenus, indicating efficient processing by caspases (Fig 2.1C, red traces). The delay between the nuclear localization and death of many of the cells suggests that the reporter is detecting activation of caspase-2, which is known to be activated in response to DNA damage (Krumschnabel et al., 2009). Notably, several surviving cells exhibit a gradual decrease in nuclear mVenus fluorescence over time, with some returning to their basal level (Fig 2.1C). This phenomenon demonstrates that the reporter can detect transient, sub-lethal caspase activation, exactly what would be required to observe non-apoptotic caspase activation in differentiating myoblasts. I then imaged the caspase reporter cell line at 15-min intervals following induction of differentiation, focusing on the period between 24 and 48 hrs after induction, as this was identified as a peak period of caspase activity detected in C2C12 lysates (Fernando et al., 2002). None of the live-cell traces from the differentiating cells (Fig 2.1C, blue traces) show the same dynamics as the

cells that respond to etoposide treatment. The peak fold increase of nuclear fluorescence also fell short of the amplitude seen in most of the responding etoposide-treated cells. The traces from the differentiating cells appear to be much noisier than those from the etoposide treatment, due to the much greater density of cells needed for differentiation. The greater density leads to much more frequent detection of out-of-focus light originating from other cells moving above or below the cell of interest. This can result in apparent increases and decreases in nuclear fluorescence, but the severity of these changes over short timescales differ from the real signal found in etoposide-treated cells, where nuclear fluorescence increases and decreases on much longer timescales. Another clear indication that there is a lack of detectable caspase activation in the differentiating cells can be seen by qualitative comparison of the morphology of their nuclear fluorescence with that of the etoposide-treated myoblasts. The nuclei of the etoposide-treated cells not only become brighter, they also display a characteristic morphology with darker spots where mVenus is presumably being excluded from nucleoli (Fig 2.1D). None of the nuclei with transiently increased fluorescence take on this appearance in differentiating cells (Fig 2.1D). Thus, my live-cell caspase reporter both quantitatively and qualitatively illustrates a lack of detectable caspase activation during differentiation.

Studies measuring caspase activity in lysates found evidence for caspase activation in differentiating myoblasts, suggesting that the live-cell reporter should also detect caspase activation at some point. On the presumption that apoptosis could account for this activity, I again imaged differentiating cells beginning 24 hrs after serum deprivation. I collected images at 3-min intervals to catch the rapid dynamics of apoptotic caspase activation, and I

identified several cells that have increased nuclear fluorescence immediately prior to detachment and death (Fig 2.2A). Images of one of these cells undergoing apoptosis show the rapidity with which the cells transition from baseline to detached and apoptotic (Fig 2.2B). In sum, my live-cell imaging results illustrate that all of the detectable caspase activation in differentiating myoblasts is associated with apoptosis.

One alternate interpretation of my results is that the live-cell reporter is not capable of detecting the level of caspase activity present in differentiating myoblasts. As stated above, I worked to optimize the sensitivity of the reporter, and its design should allow it to integrate even low amounts of activity over an extended period of time through gradually increasing nuclear fluorescence. Thus, any caspase activity would have to be incredibly low to avoid detection. While I cannot rule out this possibility, it seems implausible and also risky, given the potential detrimental effects of a sub-lethal effector caspase activation (Albeck et al., 2008; Ichim et al., 2015). The most plausible explanation for the lack of detection is that interactions between active caspases and their myogenenic substrates are being specifically mediated such that no other potential substrates are cleaved in measurable quantities; however, in this scenario it is unlikely that 20μM Z-DEVD-FMK would be sufficient to inhibit the caspase activity (Fernando et al., 2002). Thus, though I cannot meet the difficult standard of proving a negative, the most likely interpretation of my results is that there is no cell-autonomous caspase activation in C2C12s that have been induced to differentiate by serum deprivation.

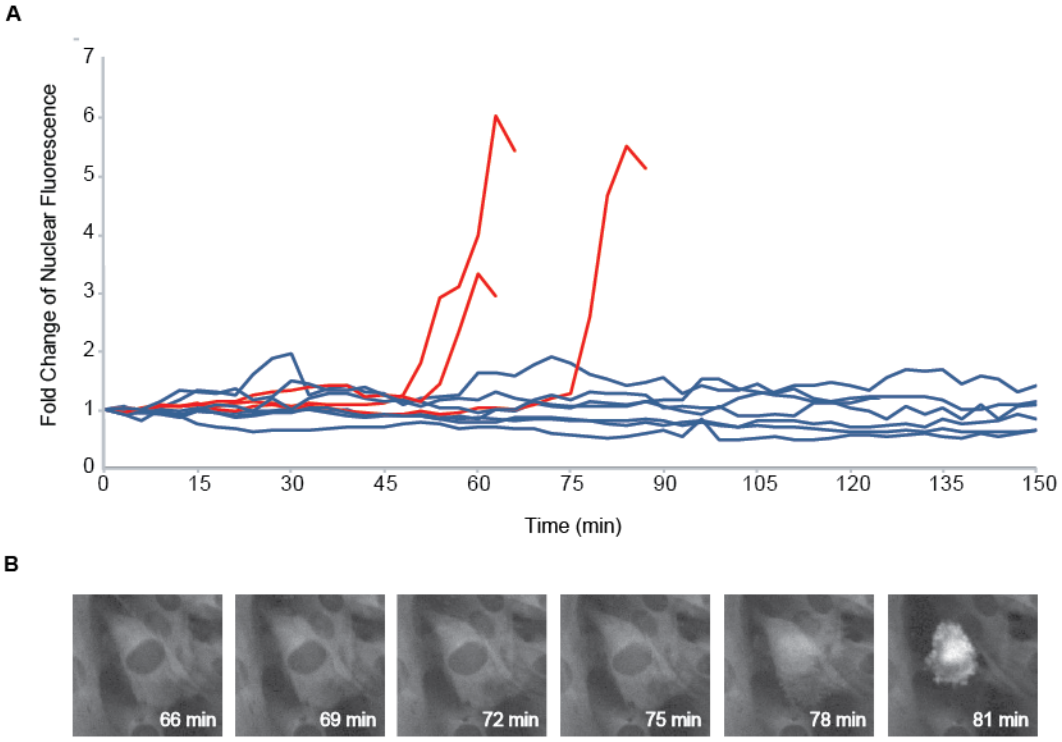

Figure 2.2: Apoptotic caspase activation is detected in differentiating myoblasts by a live-cell caspase reporter A) Single-cell traces of relative nuclear fluorescence of C2C12 cells expressing live-cell caspase reporter imaged 24 hours following induction of differentiation by serum deprivation. Traces from apoptotic cells (red) show a rapid increase in caspase activity in the 10 minutes leading up to apoptosis, in contrast to non-apoptotic cells (blue) where the nuclear signal shows only noise. Representative traces from one experiment. B) Sequential images taken at 3 minute intervals of a C2C12 cell expressing the live-cell caspase reporter undergoing apoptosis. Small increases in nuclear fluorescence give way to a rapid burst of reporter cleavage and mVenus nuclear localization.

2.3 Inhibition of caspases during myoblast differentiation results in a large population of UNDEAD cells

If, as suggested by the above experiments, there is no cell-autonomous caspase activation in differentiating myoblasts, then there must be an alternative explanation for why caspase inhibition impedes myogenesis. Before exploring these alternatives, I wanted to make sure that the inhibition of myogenesis by caspase inhibitors was actually the result of caspase inhibition and not an off-target effect. To this end, I induced C2C12 cells to differentiate in the presence of either the pan-specific caspase inhibitor Q-VD-OPh (QVD) or the closely related control compound Q-VE-OPh (QVE) (Fig 2.3A). This control substitutes aspartic acid (D) with glutamic acid (E), which, while similar, binds much less strongly to the caspase active site (Poreba et al., 2017), making it substantially worse at inhibiting caspases. After 5 days of differentiation, I quantified the differentiation efficiency of cells in each condition using the fusion index (Fig 2.3B). I found that a high concentration of QVD was able to significantly reduce the fusion index, while the QVE-treated cells differentiated as efficiently as controls (Fig 2.3C). This result strongly implies that the inhibition of myogenesis is an on-target effect of the caspase inhibitor.

My results – that caspase activation is necessary for the normal differentiation of myoblasts and that there is no detectable caspase activation in non-apoptotic cells – beg the question: is it the apoptotic function of caspases that is necessary for normal myogenesis? A significant number of myoblasts undergo apoptosis in the first 48 hrs following serum deprivation, but this is prevented by treatment with QVD. Since active

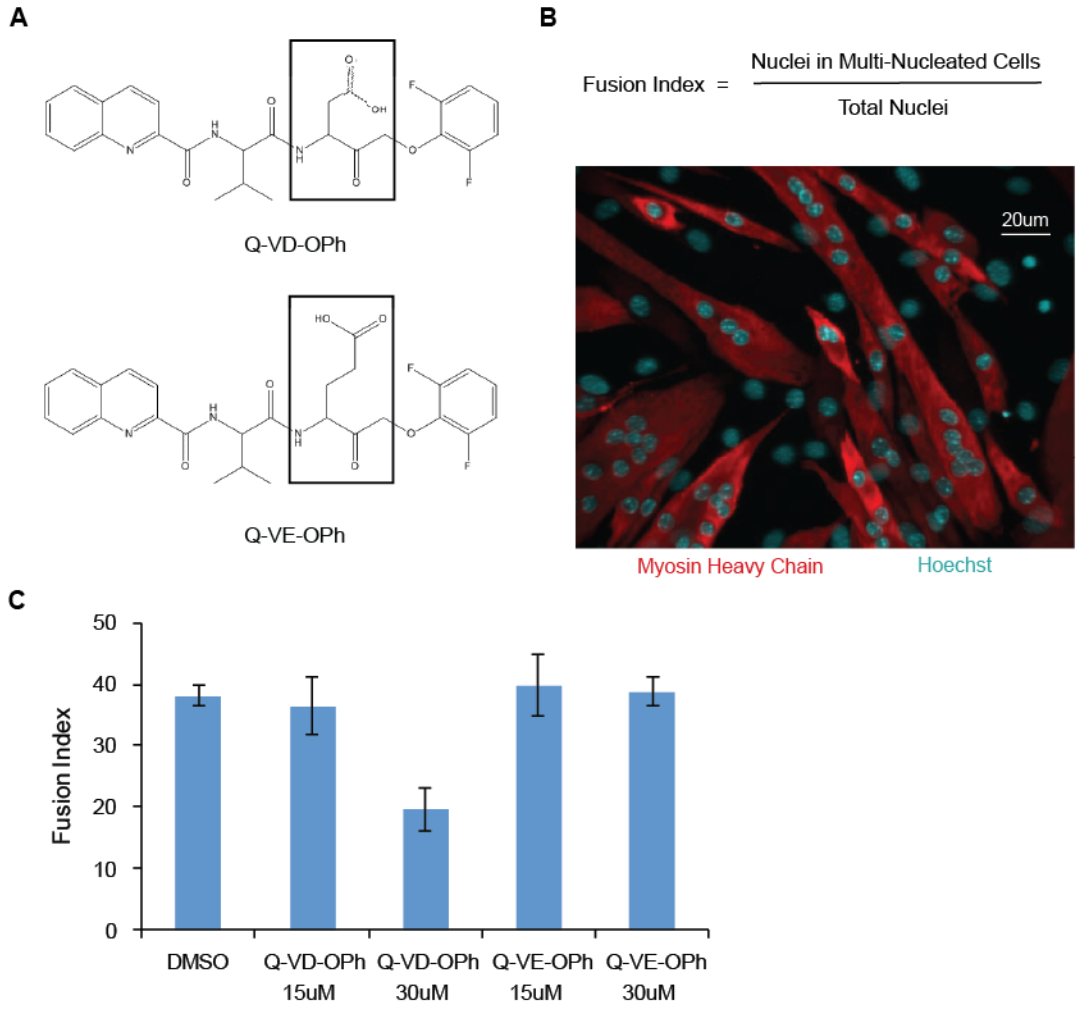

Figure 2.3: Inhibition of myoblast differentiation is not an off-target effect of caspase inhibitors
A) Structure of the caspase inhibitor Q-VD-OPh (top) and its control compound Q-VE-OPh (bottom). Boxed amino acids are the aspartic acid (top) and glutamic acid (bottom) that represent the only difference between the compounds. Despite the similar chemistry of theses two amino acids, caspases cleave after aspartic acid much more efficiently, granting excellent specificity to Q-VD-OPh. B) Quantification of myoblast fusion is done using the fusion index. Images of differentiated cells stained for myosin heavy chain, as shown, can be used to determine which Hoechst-stained nuclei are in multi-nucleated vs. mono-nucleated cells. From these counts, the fusion index can be calculated using the given equation. C) Fusion index measurement of C2C12 cells differentiated by serum deprivation for 5 days with the indicated treatment. A 30uM dose of Q-VD-OPh is able to significantly reduce the fusion index, while the same dose of Q-VE-OPh has no effect, indicating that inhibition of differentiation results from an on-target effect of the inhibitor. Bar chart shows the mean +/- SEM of 3 independent experiments.

caspase-9 can be detected in differentiating myoblasts, but not caspases-8 or -10 (Murray et al., 2008), it is likely that this cell death is the result of activation of the intrinsic apoptosis pathway. If so, there are major potential ramifications for the myoblast population following caspase inhibition, because every step of the signaling pathway upstream of caspase activation will still occur in a subset of cells. As illustrated in Figure 1.1, this means that MOMP (mitochondrial outer membrane permeabilization) should still happen, making these cells very distinct from their neighbors.

Studies have shown that there are multiple potential fates for cells that have undergone MOMP under conditions of caspase inhibition. In the majority of observed cases, that fate is eventual death via a process termed caspase-independent cell death (CICD) (Tait et al., 2010). The ultimate cause(s) of CICD are not well understood, but it can likely be explained by the loss of mitochondrial function and/or the action of proteins released from the mitochondria. Some cells have been observed to evade CICD following MOMP, but long-term survival seems to require activation of autophagy (Colell et al., 2007) and the persistence of a few healthy mitochondria (Tait et al., 2010). Very little is known about the behavior of post-MOMP cells either prior to CICD or prior to full recovery.

I hypothesized that caspase inhibition of differentiating myoblasts could create a sub-population of cells that persist for long enough following MOMP to interfere with the differentiation process. To test this, I fixed C2C12 cells at various time points following induction of differentiation in the presence of QVD. Immunofluorescent staining for cytochrome c showed that at 36 and 48 hr timepoints it was spread diffusely through the cytoplasm and nucleus in a significant number of cells, in contrast to the normal punctate

distribution observed in unperturbed cells (Fig 2.4A). This staining indicates that the cells in question have undergone MOMP and released cytochrome c from their mitochondria. Importantly, I did not observe the same phenotype in C2C12s differentiated in the absence of a caspase inhibitor (Fig 2.4B), indicating that the appearance of this population depends not just on MOMP taking place, but also on the cells avoiding the apoptosis that would normally be rapidly triggered in the absence of caspase inhibition. Most intriguingly, I discovered that there was a population of myoblasts that completely lacked cytochrome c, and that this population grew over time (Fig 2.4A, 2.4C). This suggested that, post-MOMP, cells persist for long enough for the cytochrome c to completely degrade. In fact, after two days of differentiation, upwards of 40% of the cells had either diffuse or absent staining for cytochrome c (Fig 2.4C, right panel). Incorporating information from experiments presented below, I have dubbed these cells 'Upregulators of NF-κB Dependent on Escape from Apoptotic Death' or UNDEAD cells. Given their presence at such a high frequency, the behavior of these cells could have a major impact on the differentiation of the myoblast population.

What effect UNDEAD cells may be having on the population will depend a lot on their behavior. Are they quiescent cells with no interactions? Are they more or less normal myoblasts that participate fully in myogenesis? To get a grasp on these questions, I generated a line of C2C12s stably expressing a reporter consisting of a red fluorescent protein (RFP) targeted to the mitochondrial intermembrane space (IMS-RP; Fig 2.5A) (Albeck et al., 2008). In normally growing cells, the RFP fluorescence appears punctate and perinuclear, but following MOMP there is appearance of a diffuse fluorescent signal in the

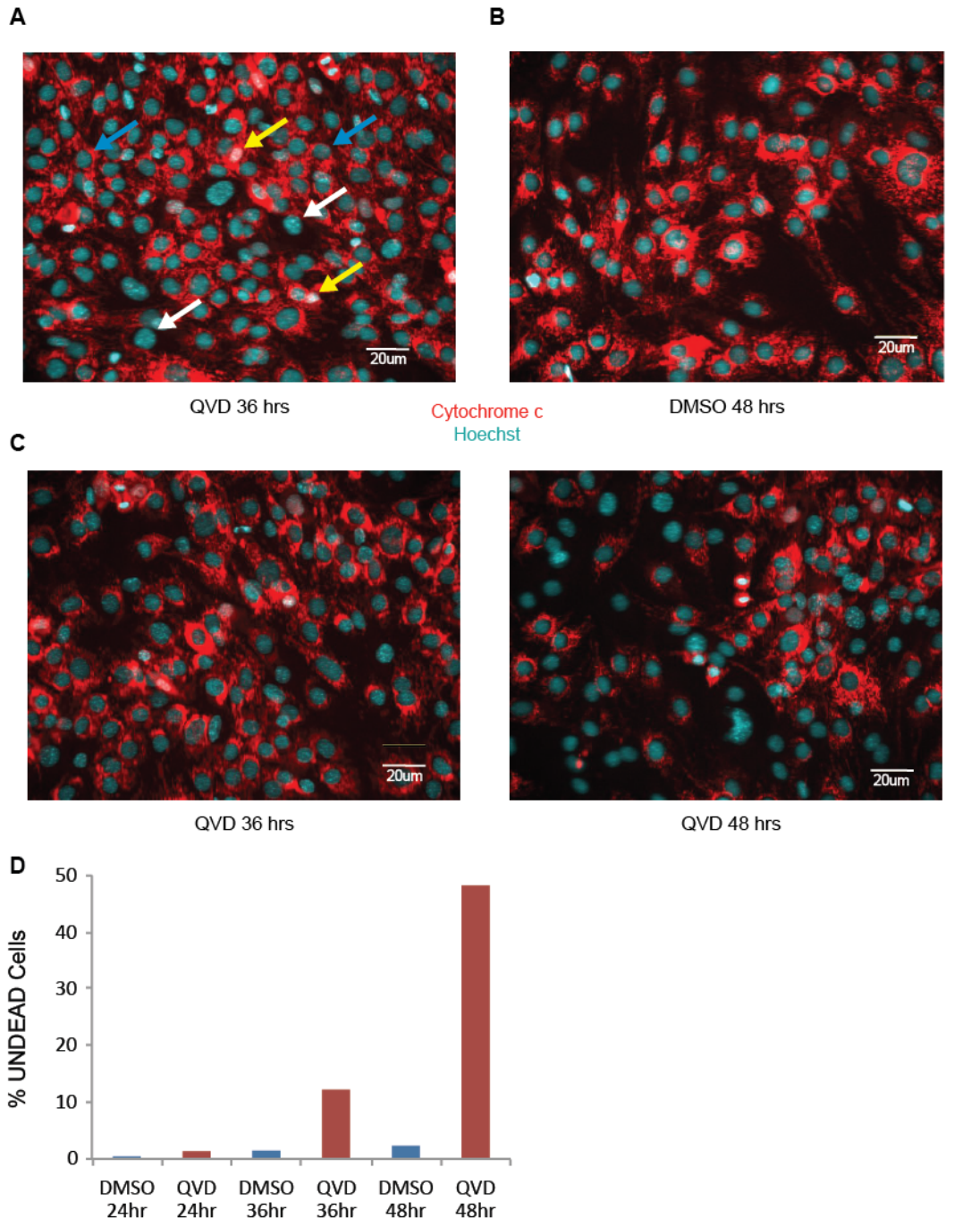

Figure 2.4: Aberrant cytochrome c staining reveals the presence of UNDEAD cells following caspase inhibition All images are representative ones of 3 independent experiments. Anti-cytochrome c staining is shown in red and Hoechst staining is shown in cyan. A) C2C12 cells differentiated for 36 hrs with 30uM Q-VD-OPh (QVD). Normal, perinuclear cytochrome c staining can be observed in most cells (blue arrows), but many also show a diffuse staining pattern (yellow arrows) or a complete absence of cytochrome c (white arrows). The cells with these last two categories of abnormal staining are UNDEAD cells that have undergone MOMP but remain alive. B) C2C12 cells differentiated for 48 hrs with DMSO. When caspase inhibitors are absent, no cells take on the UNDEAD phenotype. C) C2C12s differentiated with 30uM QVD for 36 hrs (left) or 48 hrs (right). The number of UNDEAD cells increases dramatically between 36 and 48 hrs of differentiation. D) Quantification of the percent UNDEAD cells at different timepoints from a representative experiment.

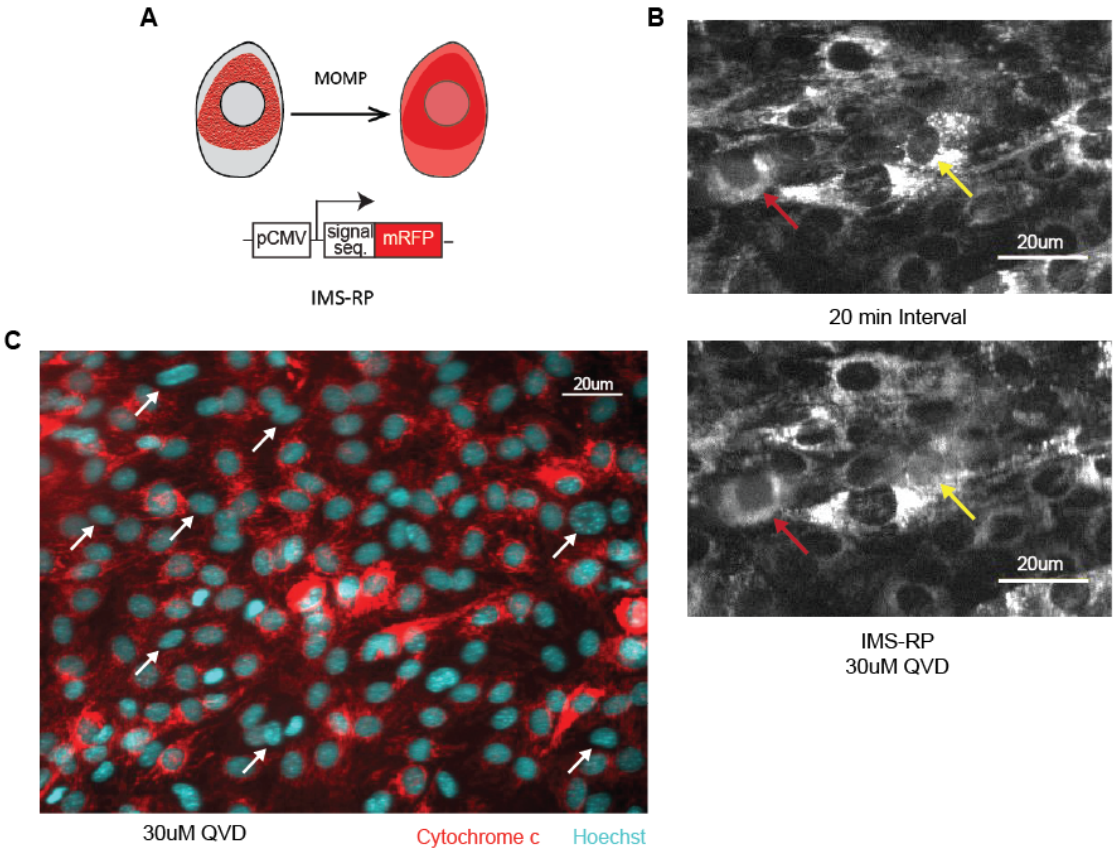

Figure 2.5: UNDEAD cells remain viable for extended periods following MOMP A) Diagram of live-cell MOMP reporter. Red fluorescent protein is localized to the mitochondrial intermembrane space until the cell undergoes MOMP and it is released into the cytoplasm and nucleus. B) Successive frames from live-cell imaging of IMS-RP-expressing C2C12 cells 23 hrs after being induced to differentiate by serum deprivation in the presence of 30um Q-VD-OPh. Red arrow indicates a cell that has recently undergone MOMP. Yellow arrow indicates a cell that undergoes MOMP in the 20 min interval between frames. C) C2C12s expressing IMS-RP were fixed after live-cell imaging and stained for cytochrome c (red) and Hoechst (cyan). White arrows indicate cells that underwent MOMP according to the live-cell reporter. All of them have an UNDEAD phenotype, confirming the accuracy of IMS-RP. Some of the indicated cells underwent MOMP more than 24 hrs preceding fixation, indicating the long-term viability of UNDEAD cells.

nucleus and the cytoplasm (Fig 2.5B). Live-cell imaging of IMS-RP expressing cells during myogenesis reveals that myoblasts undergo MOMP asynchronously and are still motile after MOMP has occurred. To validate that the reporter properly identifies MOMP, I followed live-cell imaging with fixation of the cells. Cytochrome c staining confirmed that all cells that released IMS-RP were indeed UNDEAD cells (Fig 2.5C). After observing approximately 400 UNDEAD cells over three experiments, I did not observe any dying or fusing with their neighbors. These results demonstrate that the consequences of caspase inhibition during myoblast differentiation are more complex than previously appreciated, revealing a persistent, growing sub-population of post-MOMP UNDEAD cells within the greater myoblast population. Whether this sub-population is responsible for the defect in myoblast differentiation will depend specifically on how they behave.

2.4 UNDEAD cells strongly activate NF-κB during differentiation

While insightful about the general behavior of UNDEAD cells, my observations thus far do not explain how these cells might contribute to the negative effect on myogenesis seen under conditions of caspase inhibition. Therefore, I wanted to know how the UNDEAD cells differed from their neighbors and, specifically, how these differences might hinder differentiation. I decided to address this question in the most unbiased way possible, by using RNA sequencing (RNAseq) to look for differences in gene expression between the UNDEAD and normal myoblast populations. Rather than trying to reliably sort out the two

populations for bulk RNAseq, I performed single-cell RNAseq (scRNAseq) in collaboration with the lab of Alexander Gimelbrant at the Dana-Farber Cancer Institute. I differentiated C2C12 cells for 36 hrs with either 30μM QVD or DMSO and then used the InDrop microfluidic system (Klein et al., 2015) to sort individual cells from each sample into droplets along with hydrogels containing barcoded primers (Fig 2.6A). Reverse transcription of polyadenylated RNAs was performed within the droplets and next-generation sequencing of the resulting cDNA library was done using the Illumina platform. For each sample, I obtained about 1100 unique barcodes, each corresponding to an individual cell. High-quality reads for each barcode were mapped to the mouse genome and normalized using a unique molecular identifier (UMI) sequence to ensure that each read was the result of amplification of a unique RNA. Analysis of the dataset was done using Seurat, an R package developed by the Satija lab at New York University (Satija et al., 2015).

Because I was interested in expression differences between distinct subpopulations of differentiating myoblasts, I used unbiased clustering to see what subpopulations naturally fell out of the data. I analyzed the data from the DMSO-treated and QVD-treated samples separately because I was primarily interested in how the gene expression patterns of the UNDEAD subpopulation varied from those of other cells under the same treatment condition. If the expression differences between subpopulations were subtle then the clustering analysis might not properly identify the population of interest. For said clustering

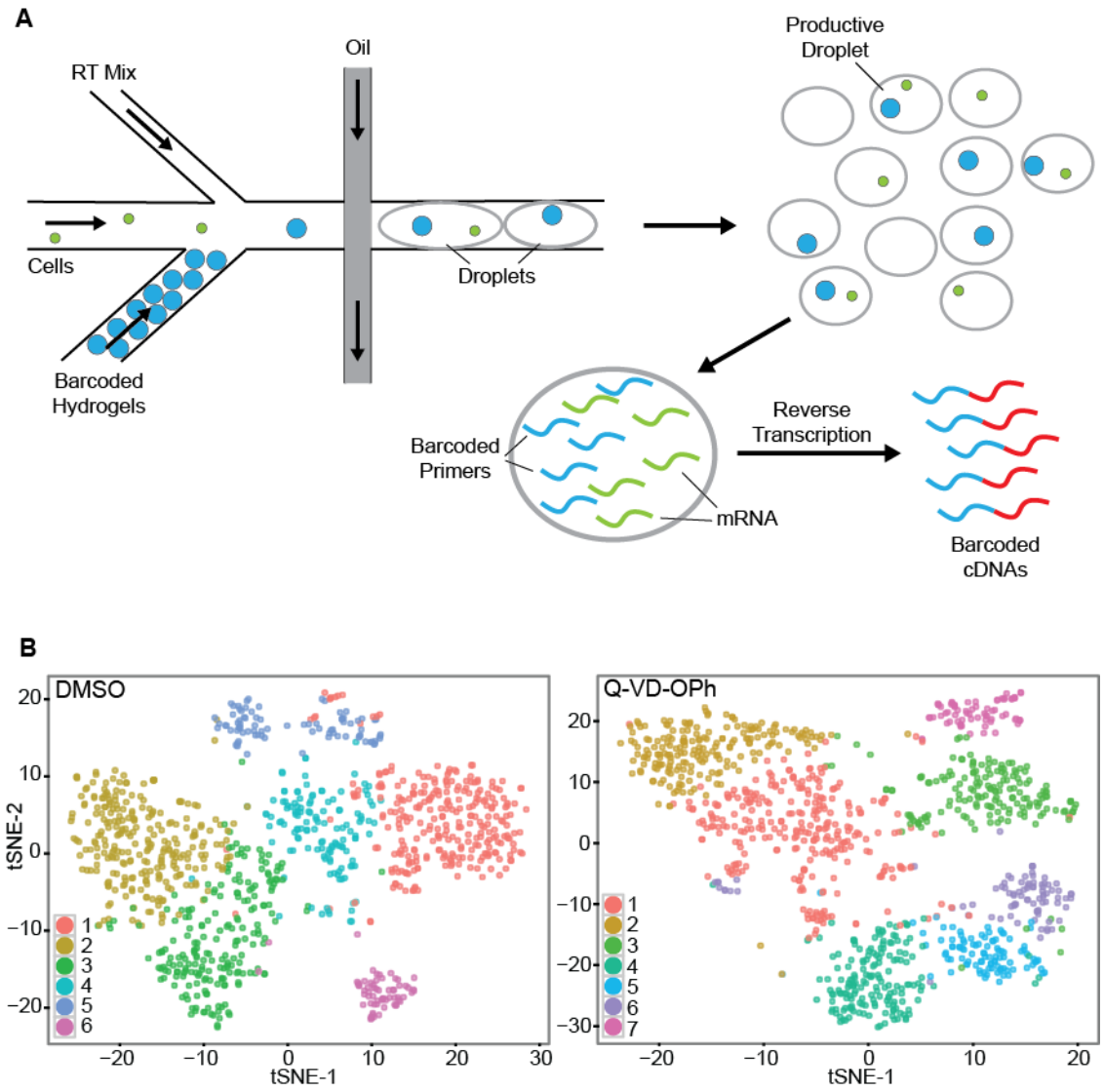

Figure 2.6: Single-cell RNAseq reveals a distinct gene expression pattern across the population of caspase-inhibited myoblasts A) To generate a barcoded cDNA library for single-cell RNAseq (scRNAseq) analysis, C2C12 cells differentiated for 36 hours with either DMSO or 30uM Q-VD-OPh were injected into a microfluidic system that sorts them into water-based droplets encased in oil. Hydrogels containing uniquely barcoded poly-T reverse transcription primers were also flowed through and productive droplets were those that included exactly one cell and one hydrogel. After collection was completed, reverse transcription was performed within the droplets which were then broken open to yield a collection of barcoded cDNA that was further amplified to generate a next-generation sequencing library. B) Single-cell sequencing data was analyzed using the Seurat toolkit. Principal component analysis was used to help perform unbiased clustering of the analyzed cells for each sample. Clusters were ordered by number of cells, largest to smallest. Above, tSNE was used to generate 2-dimensional representations of the clusters. The clusters for the two samples significantly differ with one another.

analysis, I first performed principal component analysis on the most highly variable genes in each sample to achieve linear dimensionality reduction. I then used the principal components with the highest standard deviations to cluster the cells. I used a clustering tool that uses a smart local moving algorithm (Blondel et al., 2008) to form clusters starting from a k-nearest neighbor graph. The algorithm found 6 and 7 distinct clusters, respectively, for the DMSO-treated and QVD-treated samples. To visualize the clusters in two dimensions, I used t-distributed stochastic neighbor embedding (tSNE) (Fig 2.6B). The tSNE plots give an approximate idea about the relationship between clusters, but the dimensionality reduction is non-linear and thus unreliable, so for the purposes of my analysis, tSNE has no impact on cluster assignments.

To get an idea of the reliability of the scRNAseq approach, I first analyzed the DMSO-treated sample. Cluster 6 stands out from the rest by having uniquely high expression of muscle-specific alpha actin and of myogenin, one of the core myogenic transcription factors (Fig 2.7A). Gene set enrichment analysis (GSEA) also shows that genes associated with myogenesis are enriched in this cluster (Fig 2.7B). The cells in this cluster are clearly the farthest along in the myogenic program, and it is interesting to note how stark the divide seems to be between this and other clusters. On the other end of the spectrum, cluster 5 can be seen by GSEA to be highly enriched for expression of genes related to cell cycle and cell division (Fig 2.7C), illustrating that these cells have yet to exit the cell cycle and start differentiating. That both of these populations are present simultaneously is a strong demonstration of the asynchronicity of the differentiating myoblast population that goes unnoticed when using population-based measurements.

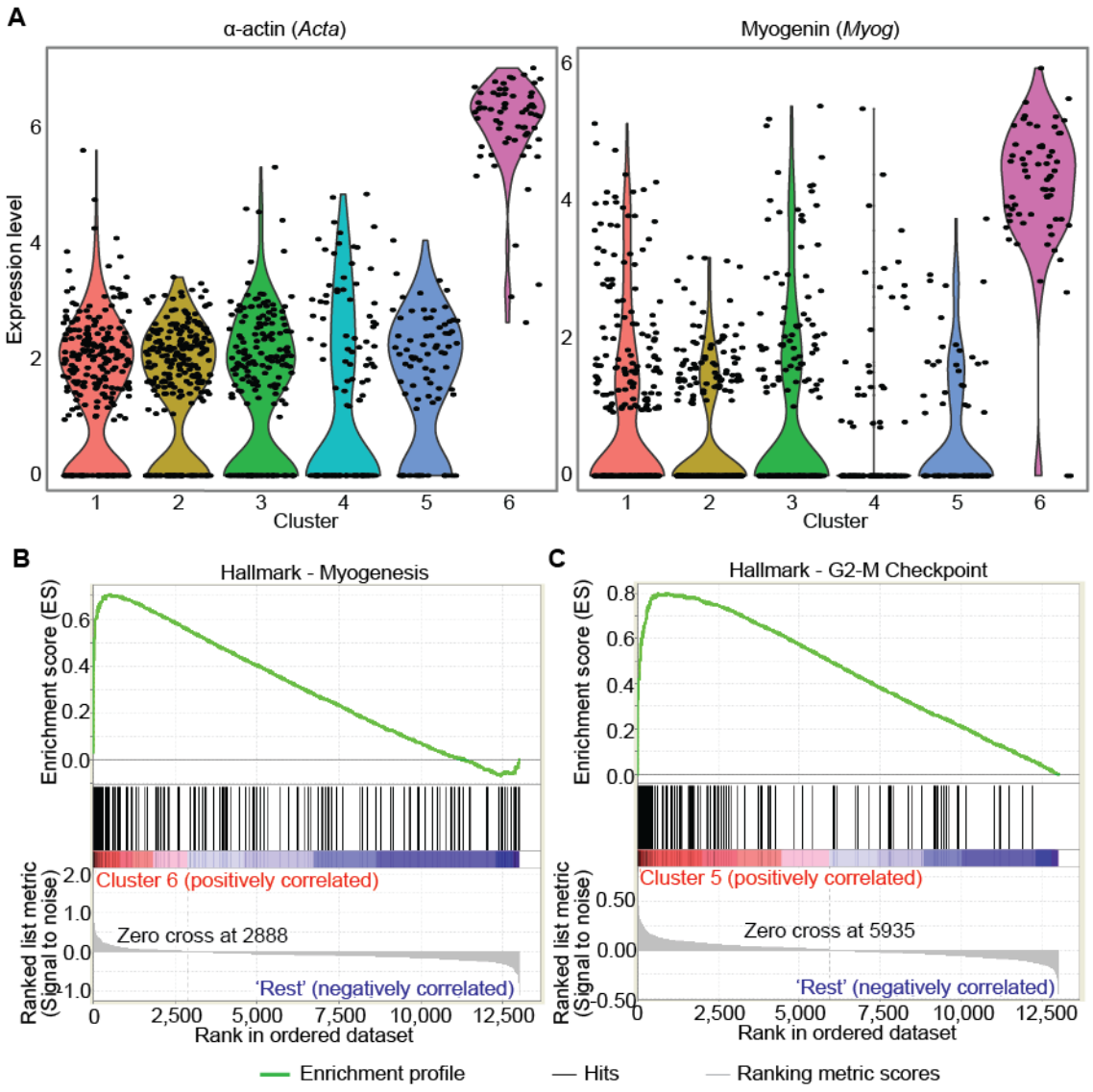

Figure 2.7: Single-Cell RNAseq clustering analysis successfully distinguishes subpopulations of differentiating myoblasts A) Violin scatter plots of expression levels of alpha-actin and myogenin show that the DMSO-treated cells grouped into cluster 6 are specifically high expressors of these two myogenic markers, indicating that these cells have advanced the farthest through the myogenic program. B) GSEA of Hallmark gene sets also shows that cells in cluster 6 are strongly enriched ($p<0.001$) for markers of myogenesis relative to the other cells in the population. C) GSEA indicates an enrichment in cluster 5 of genes expression associated with the G2-M checkpoint ($p<0.001$), suggesting that cells in this cluster have yet to exit the cell cycle.

Further analysis of the DMSO-treated sample revealed that the relative expression of genes encoding a pair of cell surface proteins drives much of the separation of the remaining clusters. The first such protein, Sca-1, is widely used as a marker of hematopoietic stem cells, but has also been observed to be upregulated in myoblasts as they exit the cell cycle (Epting et al., 2004). My results show very high expression of the gene in most cells of cluster 1 and many cells in cluster 4 (Fig 2.8A). The other protein, biglycan, is a proteoglycan that is a component of the extracellular matrix of adult muscle. Its expression has been shown to peak early in myogenesis and then gradually decrease (Casar et al., 2004). Biglycan expression is high in many of the clusters, but much lower in cluster 1 (Fig 2.8A). In fact, it appears that expression of sca-1 and biglycan is nearly mutually exclusive during the early stages of myogenesis. Cluster 4 appears to have a mix of expression levels for both, but few individual cells are high expressers of both simultaneously (Fig 2.8B). Remarkably, these markers can be used to deduce in which order the clusters are arranged during differentiation. As the cycling cells in cluster 5 start to exit the cell cycle, they upregulate sca-1 and transition to cluster 1. The cells then move to cluster 4 where they lose sca-1 expression, upregulate biglycan, and then enter cluster 2. Cells in cluster 2 then move into cluster 3, where they start to downregulate biglycan and upregulate myogenin, before finally transitioning into cluster 6. The fact that biglycan and sca-1 are cell surface proteins could provide the power to use FACS to sort out and analyze distinct subpopulations of differentiating muscle cells.

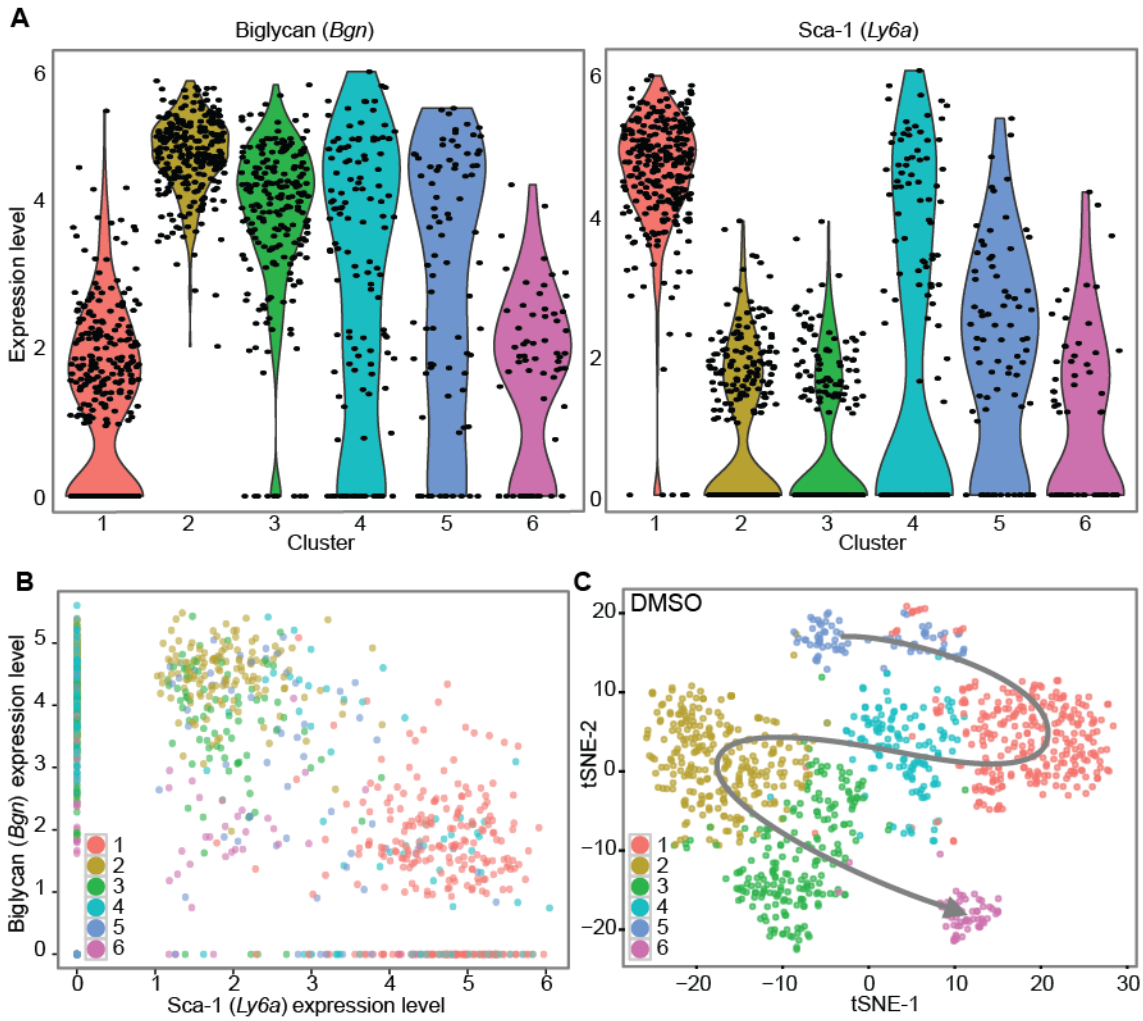

Figure 2.8: Single-Cell RNAseq reveals markers that can track the early stages of myoblast differentiation A) Violin scatter plots of expression levels of biglycan and sca-1, highly differentially expressed genes that aid in distinguishing clusters from one another. B) Plot of biglycan vs sca-1 expression shows that expression of the two genes is practically mutually exclusive, even in cells in clusters 4 and 5 that show a range of expression levels of each. C) Using the single-cell expression data of these two markers along with some information on the peak expression time of each, the path of the cells through the differentiation process can be inferred.

The expression patterns in the QVD-treated sample are drastically different from those of the control. Clustering analysis identified 7 distinct clusters rather than 6 (Fig 2.6B), and the expression patterns within the clusters are very distinct, with the following exceptions: 1) cluster 7 resembles cluster 6 of the DMSO-treated in being highly differentiated (Fig 2.9A), and 2) cluster 3 resembles cluster 5 of the DMSO-treated in being enriched for expression of proliferation genes (Fig 2.9B). The cells in clusters 1 and 2 appear to be in the intermediate stages of differentiation, but whereas the DMSO-treated cells, as noted above, could be neatly classified into stages based on sca-1 and biglycan expression, the QVD-treated cells cannot be. In fact, most of the cells have high expression of both markers (Fig 2.9C), something that was virtually unseen in the DMSO control. This makes it clear that the normal course of differentiation is being disrupted by treatment with the caspase inhibitor.

While there appears to be a general disruption of differentiation, the starkest contrast between the control and the QVD-treated is the presence of clusters 4, 5, and 6. Based on my immunofluorescence experiments, I expected to find many UNDEAD cells in the population, and the cells in these clusters are strong candidates to be them. The primary difference between cells in these clusters and the rest is the substantial decrease in expression of mitochondrial-encoded genes (Fig 2.10A). No such decrease is seen in any cells in the DMSO sample, and such a decrease would be unsurprising in cells that have undergone MOMP and lost mitochondrial potential. There could be various causes for loss of mitochondrial gene expression, but an obvious one is the removal of compromised mitochondria via mitophagy. Indeed, mitophagy has been observed in caspase-inhibited

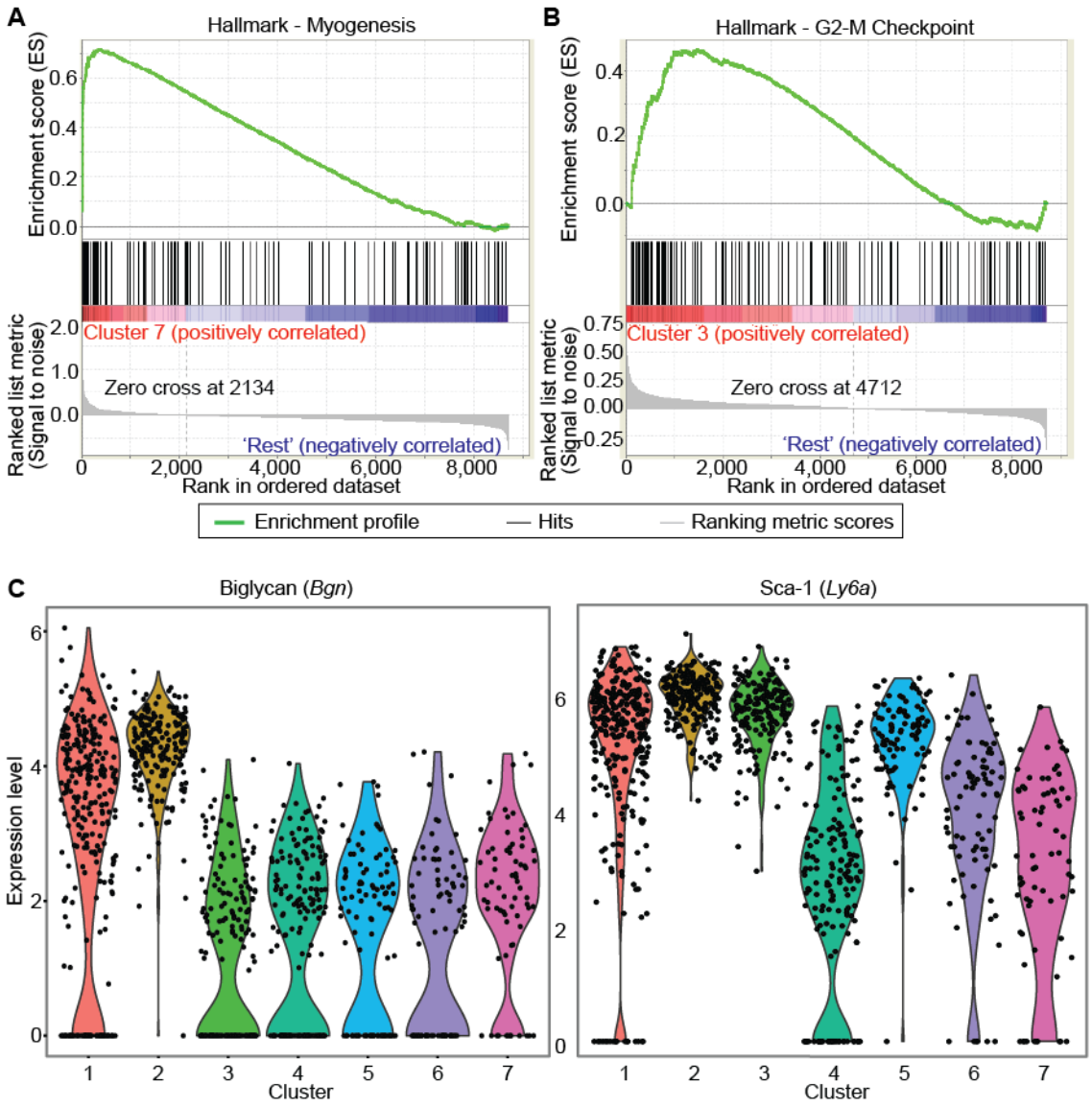

Figure 2.9: Caspase inhibition disrupts some aspects of myoblast differentiation
A) GSEA comparing cluster 7 of the QVD-treated sample with the rest of the cells from the same sample shows that it is strongly enriched for myogensis-related gene expression like cluster 6 from the DMSO-treated sample. B) GSEA comparing cluster 3 of the QVD-treated sample with the rest of the cells from the same sample shows that it is strongly enriched for G2-M checkpoint-related gene expression like cluster 5 from the DMSO-treated sample. C) Violin scatter plots of the expression of biglycan and sca-1 in the QVD-treated sample. In strong contrast to the DMSO-treated sample, many cells in the population simultaneously have either high or low expression of both genes.This suggests a generalized disruption of the differentiation process, even if a subset of the population is able to differentiate properly.

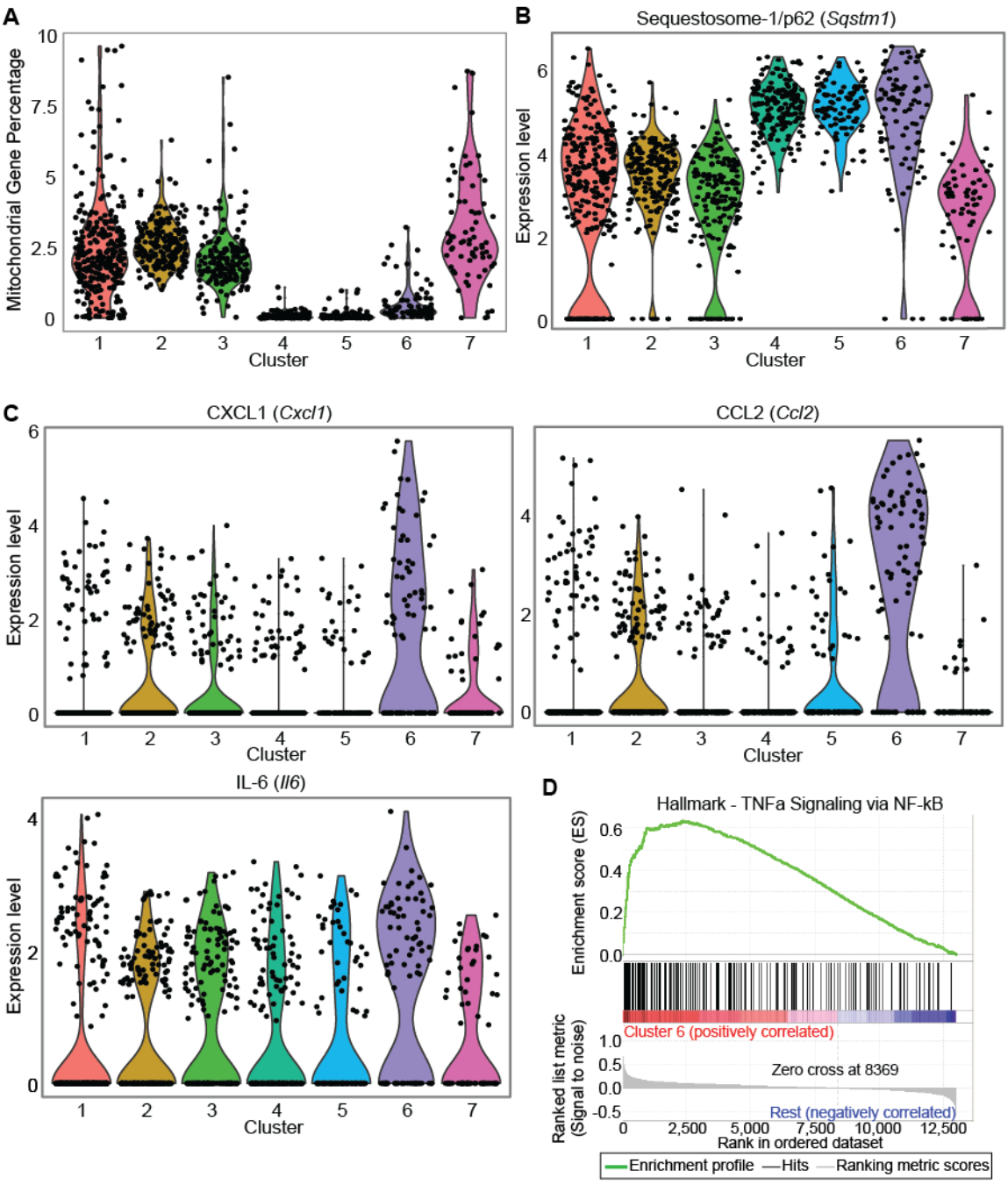

Figure 2.10: Single-cell RNA sequencing shows that UNDEAD cells specifically upregulate autophagy and that a subset also activate NF-kB signaling A) Violin scatter plot of the distributions of expression of mitochondrially-encoded genes shows that 3 clusters can be identified by abberrant mitochondrial gene expression. B) The same clusters also show specific upregulation of the selective autophagy marker p62. These clusters are likely composed of undead cells based on previous observations of post-MOMP cells and their dependence on autophagy. C) Cytokine-encoding NF-kB target genes are specifically upregulated in cluster 6, which also has the highest remaining mitochondrial gene expression of the putatitve UNDEAD clusters. D) GSEA comparing cells in cluster 6 with the rest of the population using Hallmark gene sets shows a highly significant (p<0.001) enrichment for the expression of genes associated with NF-kB signaling, confirming its activation within this subpopulation.

cells following MOMP (Colell et al., 2007) and the upregulation of sequestosome1 (p62), a marker of selective autophagy, specifically in these clusters (Fig 2.10B) indicates that mitophagy is likely happening in this instance as well. Thus, the cells in clusters 4-6, with massively decreased mitochondrial gene expression and signs of increased autophagy, are very likely post-MOMP cells that have been maintained because of caspase inhibition.

Moving forward on this assumption that clusters 4, 5, and 6 are composed of UNDEAD cells, I examined how gene expression in these cells differs from that of the rest of the population. I discovered that there is substantial upregulation of inflammatory cytokine genes in cluster 6. Prominent among these were *Ccl2*, *Cxcl1*, and *Il6* (Fig 2.10C), all of which are targets of the NF-κB transcription factor (Anisowicz et al., 1991; Libermann and Baltimore, 1990; Ueda et al., 1994). Further suggesting that NF-κB is activated in these cells, the expression of *Nfkbia*, an NF-κB target gene that encodes the NF-κB inhibitor IκBα (Haskill et al., 1991), is also specifically upregulated in cluster 6 (Fig 2.10D). Notably, cluster 6 differs from the other putative UNDEAD cell clusters in having a higher amount of mitochondrial gene expression. The most likely explanation for this is that the cells in cluster 6 are the ones that have most recently undergone MOMP (and are thus still in the process of losing expression), suggesting that activation of NF-κB signaling is triggered shortly after MOMP.

The canonical NF-κB signaling pathway can activate dozens of target genes, many of which are pro-survival and/or pro-inflammatory (Hoesel and Schmid, 2013). It can be activated as part of the innate immune system via both cytoplasmic and membrane-bound pattern recognition receptors (PRRs) that detect pathogen-associated molecular patterns

(PAMPs) during an infection. The primary subunit of canonical NF-κB is p65 (RelA), which under baseline conditions is mostly sequestered in the cytoplasm by its inhibitor IκBα. Activating signals from receptors lead to the phosphorylation and degradation of IκBα, leaving p65 free to translocate to the nucleus and induce gene expression (Karin, 1999). NF-κB signaling is usually transient, as p65 induces IκBα, which can then pull p65 out of the nucleus and return things to baseline.

To more closely examine the relationship between MOMP and NF-κB activation, I differentiated C2C12 cells for 36 hrs with 30μM QVD, then fixed them and performed immunofluorescence, staining for cytochrome c and the p65 subunit of NF-κB. I found that 87% of cells with nuclear p65 were UNDEAD cells, while UNDEAD cells made up only 12% of the overall population ($p<0.0001$ by χ^2 test; Fig 2.11A,B). This result strengthens the connection between UNDEAD cells and NF-κB target gene expression seen in the scRNAseq results and solidifies the assumption that the cells with low mitochondrial gene expression are indeed UNDEAD cells.

To further validate these findings and test my hypothesis that NF-κB activation comes shortly after MOMP, I generated a C2C12 cell line that stably expresses both the IMS-RP MOMP reporter and an mVenus-tagged p65 (Fig 2.11C). I used FACS to sort for double positives and then imaged the cells for 48 hrs following induction of differentiation by serum deprivation. I found that for the cells treated with QVD, most of cells that underwent MOMP showed nuclear translocation of p65 within a couple of hours (Fig 2.11D,E) in strong agreement with my fixed-cell data. Cells not treated with a caspase inhibitor underwent apoptosis before any p65 translocation could be observed. These

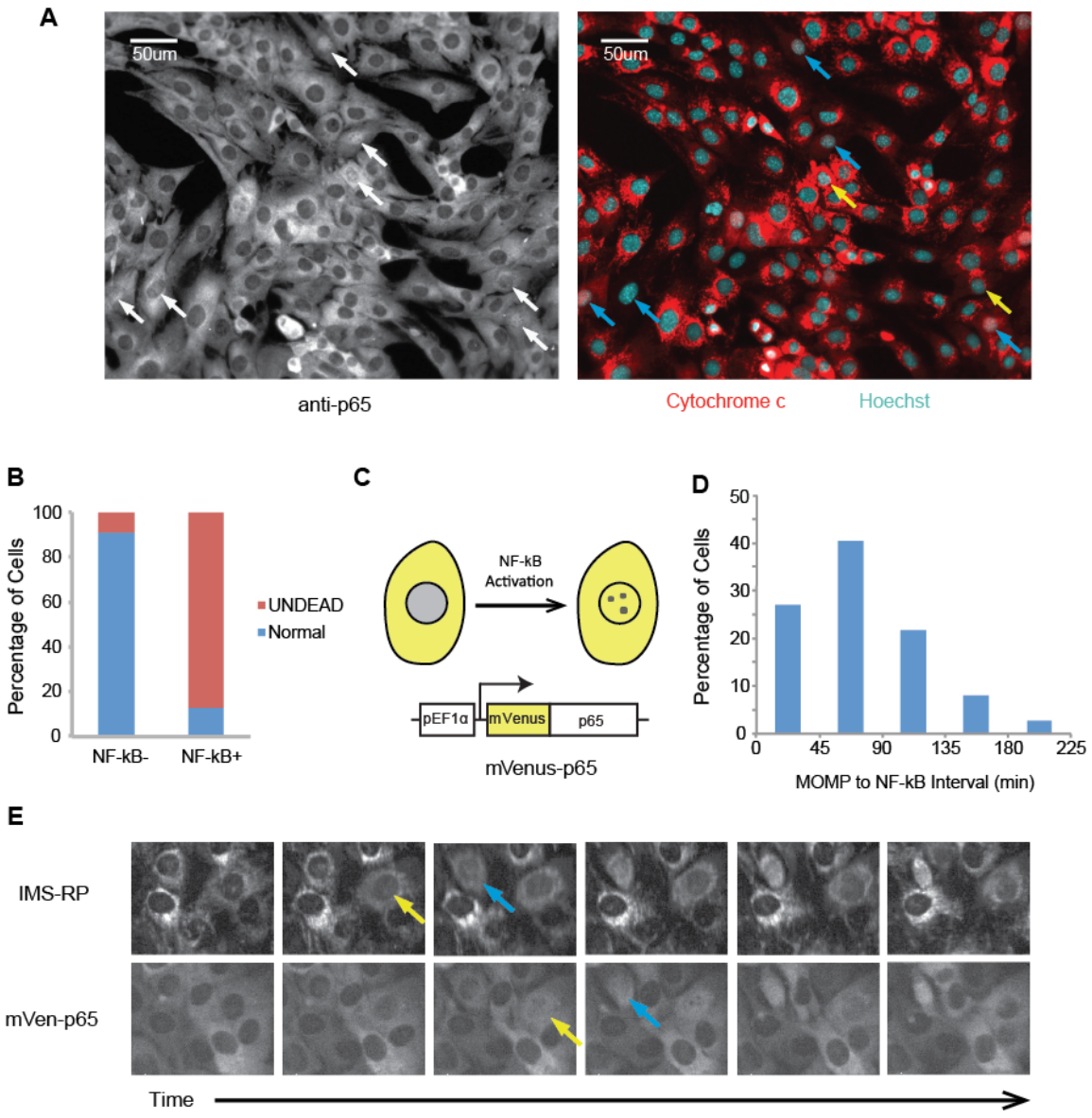

Figure 2.11: NF-kB is activated shortly after MOMP in UNDEAD cells A) C2C12 myoblasts were differentiated for 36 hrs in the presence of 30uM Q-VD-OPh. Panels show the same field of cells with staining for p65 on the left and cytochrome c (red) on the right. White arrows show cells with prominent nuclear p65. Arrows in right panel indicate whether the NF-kB positive cells are normal (yellow) or UNDEAD (blue). B) Chart indicates the distribution of normal and UNDEAD cells in each category. 87% of NF-kB+ cells show an UNDEAD phenotype. C) Diagram of NF-kB live-cell reporter consisting of an mVenus-tagged p65. Increased nuclear fluorescence indicates activation of NF-kB signaling. D and E) C2C12 cells co-expressing the IMS-RP MOMP reporter and mVenus-p65 were induced to differentiate by serum withdrawal and treated with 30uM Q-VD-OPh then imaged at 45 min intervals. D) Histogram shows the distribution of the time interval between when MOMP was observed and any observed p65 translocation. More than two thirds of cells show p65 translocation within 1.5 hrs following MOMP. E) Representative images of QVD-treated myoblasts undergoing MOMP and p65 translocation starting 48 hrs after serum withdrawal. Arrows in the upper row (IMS-RP channel) indicate the frame at which MOMP first occurs for 2 different cells. Arrows in the bottom row (mVenus-p65 channel) indicate the frame when complete nuclear translocation is achieved in those same cells. In the case of both labeled cells, p65 appears nuclear in the frame immediately following MOMP.

observations confirm my hypothesis that MOMP precedes NF-κB activation and, given the consistency of the temporal relationship between the two events, it is reasonable to speculate that there is a causal relationship between them. In sum, these results further establish UNDEAD cells as a unique sub-population of myoblasts, while also going beyond that to demonstrate that the cells that have most recently undergone MOMP are distinct from other UNDEAD cells in having a strong activation of NF-κB.

2.5 UNDEAD cells also activate type I interferon signaling during differentiation

When I examined the overall expression differences between the DMSO-treated and QVD-treated scRNAseq samples, I discovered evidence of innate immune activation beyond NF-κB. Using GSEA, I found that the interferon-alpha (IFNα) response gene set was the most upregulated set in the QVD-treated cells relative to the DMSO-treated cells (Fig 2.12A). IFNα is part of the type I Interferon (IFN) subgroup, which is composed of cytokines that are released upon infection and signal neighboring cells to increase anti-viral defenses (van Pesch et al., 2004). IFN signaling can also be anti-tumorigenic (Bhattacharya et al., 2013). At the level of individual genes, I observed that expression of *Ccl5*, a target of type I IFN signaling, was substantially increased in the caspase-inhibited sample (Fig 2.12B). Interestingly, *Ccl5* is also an NF-κB target gene, but the expression is much more evenly distributed across all of the clusters rather than being exclusively high in cluster 6. This suggests that either the gene is not being induced by NF-κB or that NF-κB-dependent

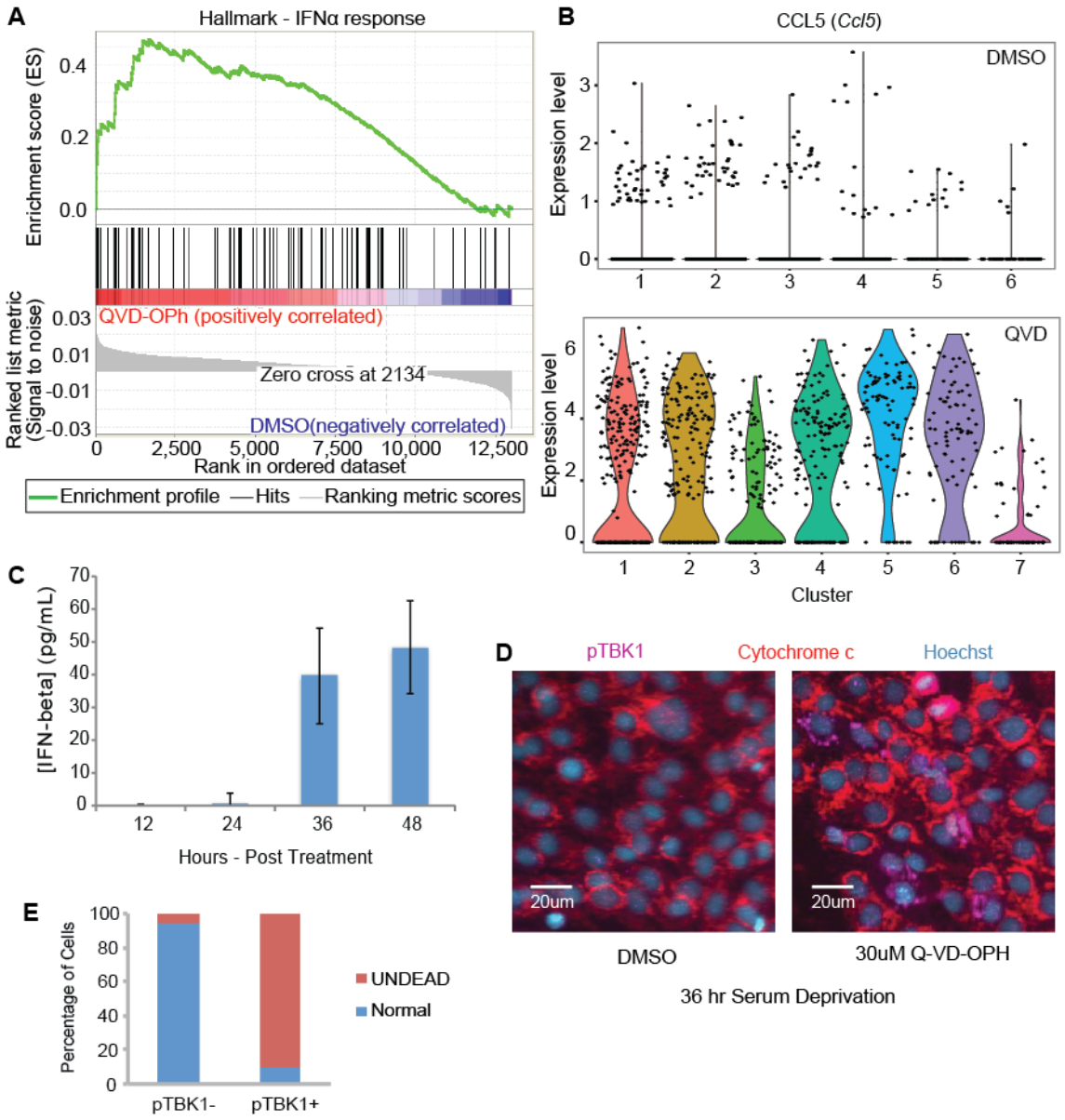

Figure 2.12: Caspase inhibition activates type I IFN signaling in differentiating myoblasts
A) GSEA comparing the two scRNAseq sample populations using Hallmark gene sets shows that there is a significant (p=0.031) enrichment for genes associated with response to IFN-alpha signaling in the sample treated with Q-VD-OPh. B) Violin plots show distribution of expression of Ccl5 across the different clusters in each sample. Ccl5 is a target of NF-kB but doesn't show enriched expression in QVD cluster 6 like other cytokines targets do. However, it is also a target of type I IFN signaling and shows signs of large scale upregulation across the population under conditions of caspase inhibition. C) ELISA of media at different timepoints following serum deprivation and QVD treatment shows that IFN-beta is secreted starting around 36 hrs following induction of differentiation. Chart displays the mean and SEM of 3 independent experiments. D) Immunofluorescence of C2C12s differentiated for 36 hrs while treated with DMSO or QVD. Staining for cytochrome c (red) and the phosphorylated (active) form of TBK1 (magenta) shows that TBK1 is preferentially activated in UNDEAD cells that lack normal cytochrome c staining. E) Chart shows the distribution of cells in the active and inactive TBK1 populations. Distributions from >300 representative cells from one of two independent experiments.

expression is getting drowned out by the uniform expression across the population that is presumably being induced by IFNs. As validation of the expression data, an ELISA assay for IFN-β found a significant concentration in the media starting 36 hrs after serum deprivation and caspase inhibition of C2C12s (Fig 2.12C).

While activation of NF-κB in post-MOMP cells is a novel discovery, secretion of type I IFN has previously been observed in mouse embryonic fibroblasts (MEFs) (Rongvaux et al., 2014; White et al., 2014), primary mouse splenocytes (White et al., 2014), and mouse peripheral blood mononuclear cells (PBMCs) (White et al., 2014) following MOMP under conditions of caspase inhibition or deficiency. The proposed explanation for this phenomenon is that, following MOMP, a significant amount of mitochondrial DNA (mtDNA) escapes from the mitochondrial matrix and enters the cytoplasm. Once there, it is recognized by the PRR cyclic GMP-AMP synthase (cGAS), which detects cytoplasmic double-stranded DNA (dsDNA). The role of cGAS has been characterized in situations where the dsDNA is the result of an infiltrating virus, and it appears to function identically in response to mtDNA. Detection of dsDNA triggers cGAS to produce cyclic GMP-AMP (cGAMP), which in turn activates the stimulator of interferon genes (STING) protein. STING then activates TANK-binding kinase 1 (TBK1), which phosphorylates and activates the transcription factors interferon regulatory factor(IRF)-3 and IRF-7, which then direct the transcription of the type I IFN genes (Abe and Barber, 2014). The similarities between these circumstances and those in my UNDEAD cells beg the question: is this same pathway getting activated in UNDEAD cells?

To address this question, I differentiated C2C12 cells for 36 hrs in the presence of 30 μM QVD and then stained for cytochrome c and the phosphorylated (and thus active) form of TBK1. I found that phospho-TBK1 was specifically present in UNDEAD cells (Fig 2.12D). About 19% of the cells showed activation of TBK1 and of these, 90% were cells with characteristic UNDEAD cytochrome c staining, a highly significant correlation ($p<0.0001$ by χ^2 test). Meanwhile, DMSO-treated populations that lacked UNDEAD cells showed almost no sign of TBK1 activation. The specificity of TBK1 activation to UNDEAD cells would seem to contradict the scRNAseq findings, which did not show disproportionate upregulation of type I IFN response genes in the UNDEAD clusters. However, this may be explained by the ability of type I IFN signaling to activate a STAT1/STAT2/IRF9 transcriptional complex that can also initiate type I IFN response gene transcription (Litvin et al., 2015). This type of positive feedback will tend to make the distribution of transcription more uniform across the population. Based on my data and evidence from the literature, I hypothesize that IFN signaling is activated in UNDEAD cells via a cGAS/STING/TBK1/IRF3 pathway initiated by mtDNA that enters the cytoplasm following MOMP and then amplified across the population by JAK-STAT signaling. Experiments to specifically test the requirement for mtDNA in this process are ongoing.

While my work shows that NF-κB activation is linked to MOMP, it is an open question whether the same general pathway is responsible for the activation of both NF-κB and IFN signaling. It seems likely, as it has been demonstrated that in other contexts cGAS

and STING are part of a pathway that activates NF-κB in response to dsDNA (Abe and Barber, 2014). However, there are many ways that NF-κB could potentially be activated, so further study will be needed to confirm whether cytoplasmic mtDNA is the ultimate trigger.

2.6 Conditioned media from caspase-inhibited, differentiating myoblasts inhibits the differentiation of naïve myoblasts

While I have established that caspase inhibition leads to the formation of UNDEAD cells that activate innate immune signaling pathways, I have yet to connect the UNDEAD cells to the differentiation defect observed when myoblasts are treated with a caspase inhibitor. Related to this, the results of my scRNAseq experiment showed increased expression of several inflammatory cytokines in UNDEAD cells (Fig 2.10C), presumably due to activation of the NF-κB pathway. There is a strong possibility that these cytokines could act as paracrine factors that could influence cells throughout the population in various ways, including inhibiting differentiation. To confirm that these cytokines are indeed secreted and to see what other cytokines might be secreted as well, I collected media from C2C12 cells after 48 hrs of differentiation in the presence of either DMSO or QVD. These samples were assayed using the Bio-Plex 23-plex mouse cytokine array to measure the concentration of 23 cytokines. Looking at the concentrations of each cytokine in the caspase-inhibited samples relative to the controls, I observed that many of the assayed cytokines were present at significantly higher concentrations under conditions of caspase

inhibition, including those whose genes were shown by scRNAseq to be upregulated in UNDEAD cells (Fig 2.13A). The cytokines that see a greater than 2-fold increase in concentration in the caspase-inhibited samples are generally thought of as pro-inflammatory.

Given my inability to detect caspase activation in differentiating myoblasts, the cause of the differentiation defect seen in response to caspase inhibition would most likely have to be cell non-autonomous. The secretion by UNDEAD cells of large quantities of inflammatory cytokines into the local environment would provide such a non-autonomous mechanism. In fact, CCL2, CCL3, CCL4, and CCL5, all members of the CC chemokine family, have been shown to have pro-proliferative effects (Yahiaoui et al., 2008), and because the trigger to begin differentiation is cell cycle exit, it stands to reason that increased proliferation should hinder differentiation. Further, my scRNAseq data confirms that my C2C12 cells express the genes corresponding to the receptors for these chemokines, making such a scenario more plausible. There is also precedent for cell non-autonomous NF-κB negatively influencing muscle regeneration (Oh et al., 2016). I therefore hypothesized that exposure to factors secreted by caspase-inhibited, differentiating myoblasts is sufficient to inhibit efficient myogenesis.

I set out to test this hypothesis with the use of conditioned media (CM). I differentiated C2C12s in the presence of either DMSO or 30 μM QVD for 48 hrs, at which time I harvested the media from each sample and filtered it to remove dead cells and debris. I then used a spin concentrator with a 3000 Da MW cutoff to remove approximately 99% of the caspase inhibitor, which would be a major confounding factor if present in the

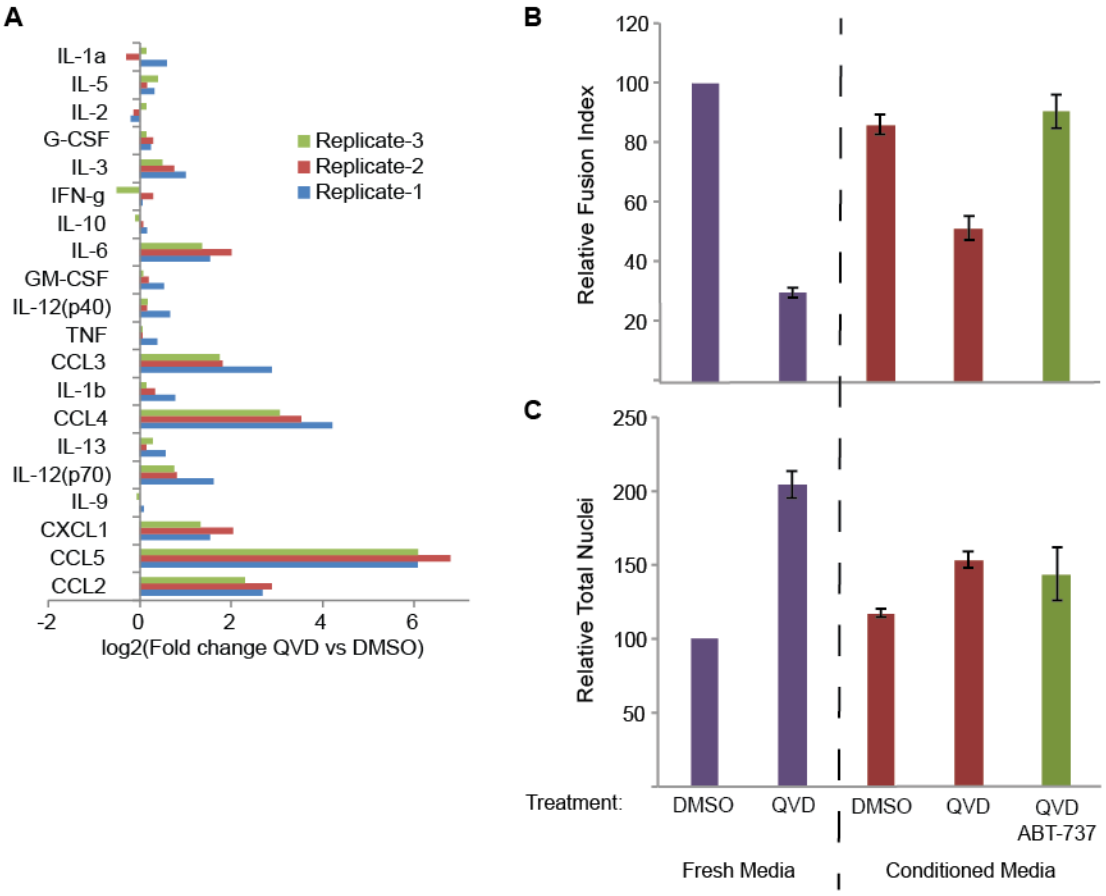

Figure 2.13: Media from caspase-inhibited differentiating myoblasts is rich in cytokines and can inhibit the differentiation of naive cells A) Measurement of 23 cytokines in media taken from differentiating C2C12 cell treated with either DMSO or 30uM Q-VD-OPh. Chart shows the fold increase in QVD-treated samples relative to DMSO-treated for 3 independent experiments. There is a large increase in the concentration of several inflammatory cytokines. B,C) C2C12 cells were differentiated for 5 days with either fresh media supplemented with DMSO or QVD, or with conditioned media that was taken either from cells differentiated for 48 hrs with DMSO or QVD, or from cells treated with QVD and a 0.7uM dose of the MOMP-inducing drug ABT-737. The fusion index (B) and the total nuclei (C) were measured at the end of 5 days. Conditioned media from QVD-treated cells was sufficient to inhibit differentiation, though no inhibition was seen from the CM taken from ABT-treated cells, despite the large number of UNDEAD cells in their population. Results show mean +/- SEM of 4 independent experiments.

CM. Both samples were concentrated 10-fold, in the process of which the drug was removed alongside the bulk of the media. The samples were then returned to their starting volumes with fresh serum-free media and the process was repeated an additional time. I then took the resulting CM, mixed it with equal parts fresh differentiation media and used it to treat naïve C2C12 cells. After 5 days, the fusion index was scored relative to controls treated with fresh media.

I discovered that, as expected, the CM from the cells treated with caspase inhibitor had a significant negative effect on myogenesis, whereas CM from DMSO-treated cells was only mildly inhibitory relative to fresh media with DMSO (Fig 2.13B). As mentioned above, several of the secreted cytokines that should be present in the CM are pro-proliferative. To see if there was evidence of an increase in proliferation, I also compared the total number of nuclei present in each sample at the end of the 5 days of differentiation. I found that there were significantly more nuclei when the CM originated from caspase-inhibited cells (Fig 2.13C), consistent with an increase in proliferation. These results support a model whereby UNDEAD cells release cytokines that both promote the proliferation and inhibit the differentiation of neighboring myoblasts. Importantly, my results also strongly contradict the previously put forth model wherein caspase activation is required cell autonomously for myoblasts to differentiate properly, by showing that the presence of factors released in response to caspase inhibition is sufficient to inhibit differentiation.

To more cleanly and directly test the effects of factors secreted from UNDEAD cells, I generated a population of them outside of the context of differentiation by treating C2C12s with QVD and the Bcl-2 antagonist ABT-737. This drug has been shown to promote MOMP

(Kroemer et al., 2007), so when combined with a caspase inhibitor, it efficiently generates UNDEAD cells (Rongvaux et al., 2014; White et al., 2014). The treatment of the cells was done using serum-free media, which was harvested after 48 hrs. The drugs were removed as described above, and fresh horse serum was added before using the media to treat naïve cells. Interestingly, there was no significant reduction in the fusion index for the cells treated with this media relative to those treated with DMSO, but there was an increase in the total number of nuclei (Fig 2.13C). These results suggest that the pro-proliferative effects of factors secreted from UNDEAD cells are much more robust than the anti-differentiation effects, although it is not immediately clear why this is the case.

2.7 The cytokine secretion and inhibition of myoblast differentiation resulting from caspase inhibition is MOMP-dependent

Thus far, my interpretation of my results has assumed that UNDEAD cells were directly responsible for the inhibition of differentiation, the presence of cytokines in the media and the inhibitory effects of CM. As confirmation of these assumptions, I sought to prevent the formation of UNDEAD cells when I treat myoblasts with a caspase inhibitor. Thus, I made C2C12 cell lines that stably overexpressed either Bcl-xL or Bcl-2 (Bcl-xL-OE; Bcl-2-OE), both of which are anti-apoptotic members of the Bcl-2 family. Increased expression of these proteins has been shown to reduce the likelihood of MOMP (Yip and Reed, 2008). Thus, sufficient overexpression of these two proteins should prevent the formation of

UNDEAD cells. Both genes were introduced into cells by retroviral infection, and both were part of constructs that also co-expressed GFP from an internal ribosome entry site (IRES) (Cheng et al., 2001) (Fig 2.14A). Cells positive for high levels of GFP were isolated by FACS sorting and used for all experiments. The overexpression of Bcl-xL and Bcl-2 was confirmed by western blot (Fig 2.14B), with Bcl-xL showing especially high levels of expression.

When differentiated alongside wild-type C2C12s, both the Bcl-xL-OE and Bcl-2-OE cells showed an increase in the fusion index under conditions of DMSO treatment (Fig 2.14C). This result is interesting, since a previous study found that Bcl-xL overexpression lead to a decrease in the fusion index. That study speculated that they got their result because MOMP is required for a pro-differentiation, non-apoptotic caspase activation; however, they found no signs of mitochondrial depolarization or other indicators of MOMP in normally differentiating cells. I hypothesize that my overexpressors differentiate better than wild-type because the decrease in dead cells leads to a higher cell density, and cell density positively correlates with fusion efficiency (Tanaka et al., 2011). Perhaps this positive effect overshadows a negative one that I then miss, but even so, the robustness of the previously published observation is called into question, making it appear unlikely that there is any need for MOMP for efficient myoblast differentiation.

Even if it appears that there is no MOMP-dependent, non-apoptotic caspase activation required for myoblast differentiation, theoretically there could be one that was MOMP-independent. However, I observed that the negative effect of caspase inhibition on differentiation is severely blunted by overexpression of both Bcl-xL and Bcl-2 (Fig 2.14C). This result is not consistent with a MOMP-independent, pro-differentiation caspase

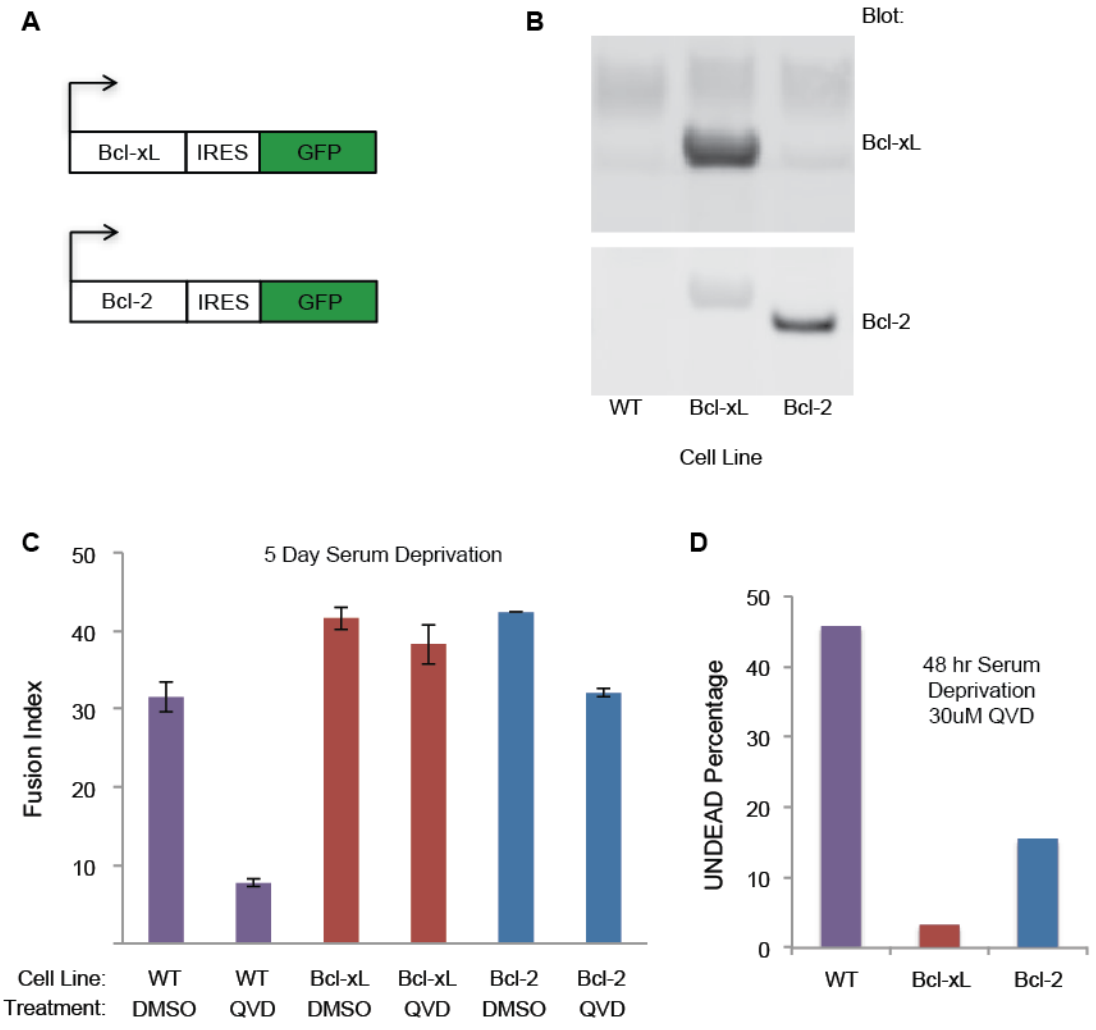

Figure 2.14: Anti-apoptotic Bcl-2 protein overexpression prevents UNDEAD cell formation and blocks caspase-inhibitor-mediated inhibition of myoblast differentiation A) Schematics of Bcl-xL and Bcl-2 overexpression constructs, which both express GFP off of an IRES. B) Western blot of Bcl-xL-OE and Bcl-2-OE cell lines following infection and sorting for high GFP expressors. C) Fusion index measurement of WT, Bcl-xL-OE, and Bcl-2-OE cell lines after 5 days of serum deprivation. Fusion of Bcl-xL-OE cells is not significantly affected by caspase inhibition. Bcl-2-OE cells are modestly inhibited. Resuslts reported as mean +/- SEM of 4 independent experiments. D) UNDEAD cells were scored for 3 cell lines following 48 hrs of differentiation with 30uM QVD. The percentage of the population scored as UNDEAD is shown for a representative experiment. Virtually no UNDEAD cells are found in the Bcl-xL-OE population, which is also the most resistant to caspase inhibition when differentiating.

activation but is consistent with the idea that the generation of UNDEAD cells is the root cause of the inhibition of differentiation. It is interesting to note that there is still a small negative effect on differentiation in both overexpressor cell lines that would be difficult to explain if UNDEAD cells were absent from the population. However, looking 48 hrs after the induction of differentiation, I find that there is still a small population of UNDEAD cells in the Bcl-xL-OE cells and a moderately sized one in the Bcl-2-OE cells (Fig 2.14D). Comparing the measurements for each cell line, there is a clear negative correlation between the size of the UNDEAD population and the fusion index following caspase inhibition, strongly supporting a model wherein UNDEAD cells drive the inhibition of myoblast differentiation.

As part of an effort to interrogate how UNDEAD cells might inhibit differentiation, as well as to characterize the UNDEAD cells more generally, I again used the Bio-Plex cytokine array to see how blocking UNDEAD cell formation affects the profile of secreted cytokines. Media from wild-type, Bcl-xL-OE, and Bcl-2-OE cells was harvested 48 hrs after induction of differentiation in the presence of either DMSO or QVD. The cytokine array results for these samples illustrate that the increase in secreted cytokines seen in caspase-inhibited, wild-type C2C12s is almost entirely dependent on the presence of UNDEAD cells, as there was almost no increase in cytokine levels in the Bcl-xL-OE cells and much lesser increases in the Bcl-2-OE cells (Fig 2.15A).

I hypothesized that the cytokines secreted from UNDEAD cells are a major cause of both the pro-proliferation and anti-differentiation effects triggered by CM originating from caspase-inhibited myoblasts. Having found that the concentration of cytokines is greatly

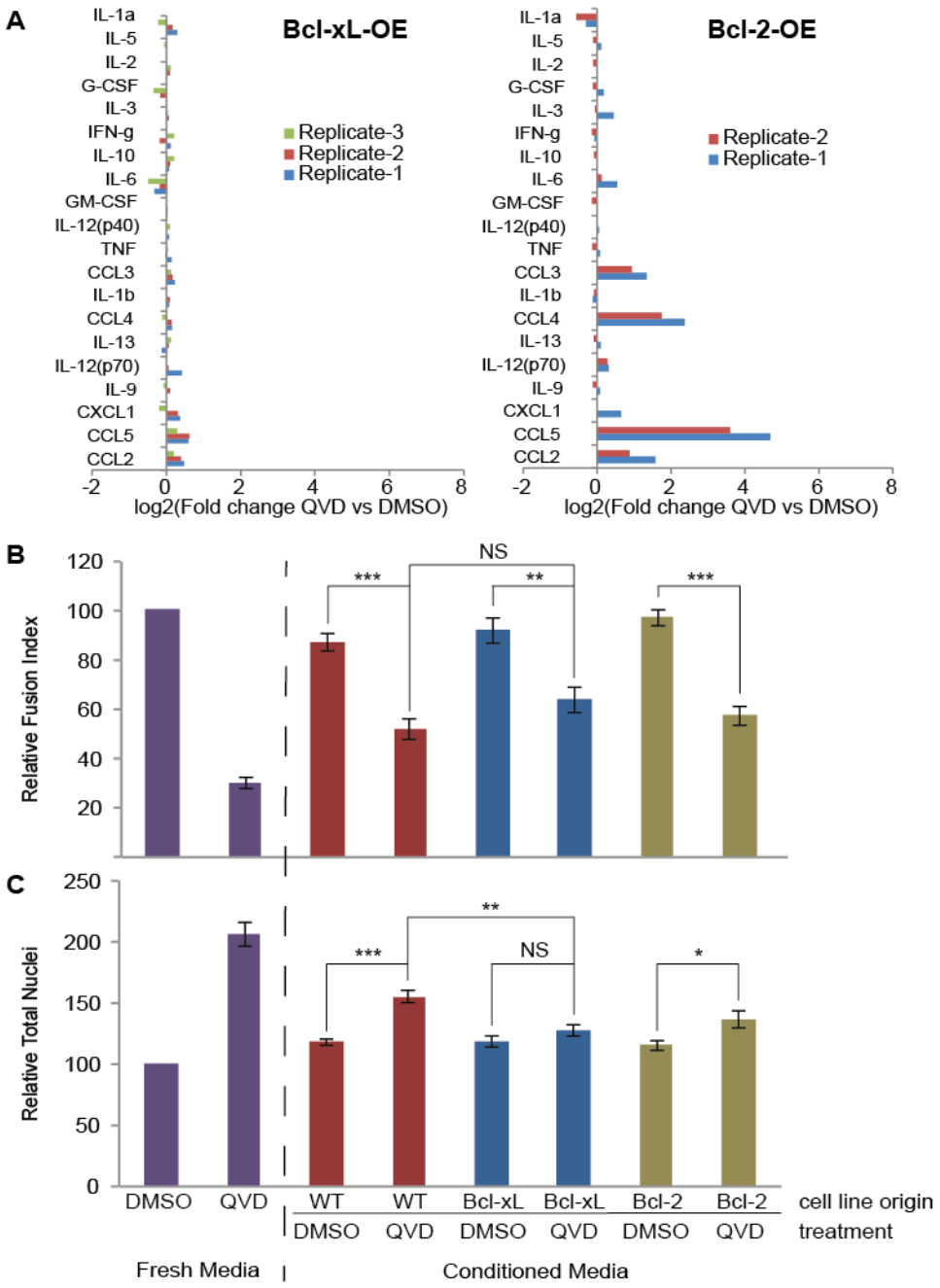

Figure 2.15: UNDEAD cells are responsible for cytokine secretion and the pro-proliferative effects of conditioned media A) Independent measurements of 23 cytokines as in Figure 2.13A in media taken from Bcl-xL-OE and Bcl-2-OE cell lines. In the Bcl-xL-OE line that virtually lacks UNDEAD cells, caspase inhibition results in almost no increase in cytokine secretion. In the Bcl-2-OE cells with an intermediate number of UNDEAD cells, there is a significant increase in secretion of some CC chemokines, but to a lesser extent than from WT cells. B,C) Results of a conditioned media experiment as in Figure 2.13B and C. B) CM derived from Bcl-xL-OE and Bcl-2-OE cells after treatment with QVD shows nearly the same ability to hinder myoblast differentiation as CM from WT cells. C) looking at total nuclei, the CM from caspase-inhibited Bcl-xL-OE cells shows no significant pro-proliferative effect. Results show mean +/- SEM of 4 independent experiments. * = $p<0.05$; ** = $p<0.01$; *** = $p<0.001$; NS = not significant. p-values calculated using student's t-test.

reduced in the CM taken from Bcl-xL-OE and Bcl-2-OE cells, I tested to see what effect this CM has on differentiating wild-type C2C12s. I found that the total number of nuclei present after 5 days of differentiation is not significantly increased in C2C12s treated with CM from QVD-treated Bcl-xL-OE cells relative to those treated with CM from DMSO-treated Bcl-xL-OE cells (Fig 2.15C). In contrast, CM from WT cells treated with QVD significantly increased the total nuclei. While these results do not rule out the possibility that the pro-proliferative effect of the CM is due to the presence or even the absence of some non-cytokine factor(s), the positive correlation between the concentration of cytokines in the media and the degree of proliferation as well as the documented pro-proliferative effects of the cytokines in question, strongly suggests that these cytokines are mediating the increased proliferation. Somewhat unexpectedly, I discovered that the CM taken from caspase-inhibited Bcl-xL-OE and Bcl-2-OE cells is nearly as inhibitory of myoblast fusion as the CM from WT C2C12s (Fig 2.15B). In fact, the differences in the fusion indices between these three conditions are not statistically significant.

Taking these results with those of my previous experiments, I can conclude 1) that inhibition of myoblast differentiation by caspase inhibitors depends on the presence of a significant number of cells capable of undergoing MOMP and becoming UNDEAD cells; 2) that UNDEAD cells are the source of the inflammatory cytokines released under conditions of caspase inhibition; 3) that these cytokines are responsible for the increased proliferation of myoblasts exposed to CM from caspase-inhibited cells; 4) that these cytokines are not

the primary cause of the inhibition of differentiation resulting from CM treatment; and thus 5) that the full explanation for how caspase inhibitors cell non-autonomously inhibit myoblast differentiation is a complex one.

2.8 Discussion

I have sought to address the counterintuitive reports that apoptotic caspases are active and serving a non-apoptotic function in myogenesis. To this end, I demonstrated a lack of detectable non-apoptotic caspase activation in differentiating myoblasts using a live-cell caspase reporter. I also showed that media conditioned by caspase-inhibited, differentiating myoblasts is sufficient to hinder the differentiation of C2C12s to nearly the extent of direct treatment with a caspase inhibitor. Furthermore, I demonstrated that prevention of MOMP is sufficient to rescue the differentiation defect triggered by caspase inhibition. In sum, these results strongly refute the possibility of a non-apoptotic caspase activation in differentiating myoblasts.

Though I have refuted the previous model explaining how caspase inhibition causes myoblasts to differentiate poorly, I am still left to ask what the full mechanism is by which caspase inhibition hinders myoblast differentiation. Insight towards an answer to this may come from the fact that CM from Bcl-xL-OE cells treated with QVD had an inhibitory effect on differentiation, while there was no inhibitory effect from CM taken from WT UNDEAD cells created by QVD and ABT-737 treatment. This result suggests that there may be release

of one or more inhibitory factors in response to caspase inhibition that are only released in the context of differentiation, independent of the presence of UNDEAD cells. Careful study of the composition of conditioned medias generated under a variety of treatments may be able to isolate one or more factors that drive the observed inhibition.

Another potentially important observation concerning the mechanism by which differentiation is inhibited is that the number of UNDEAD cells in the population at 48 hrs following serum deprivation and beyond is greater than the number of cells that normally die by apoptosis. This implies that the inhibitor is inducing some myoblasts to undergo MOMP, creating additional UNDEAD cells, and/or that UNDEAD cells induce neighboring cells to undergo MOMP. These scenarios can potentially be addressed by precise quantitation of apoptosis induced by different treatments and CMs as well as by careful live-cell observations of UNDEAD cell formation using the IMS-RP live-cell MOMP reporter to see if new UNDEAD cells are more likely to form near existing ones. Demonstrating the precise mechanism responsible for the inhibition of differentiation would further repudiate of the notion that apoptotic caspases have a non-apoptotic function in myoblast differentiation.

My experiments have also lead to the discovery that inhibiting caspases in differentiating myoblasts leads to the generation of an UNDEAD cell population that evades caspase-independent cell death for an extended period. Through immunofluorescence, live-cell microscopy, and scRNAseq, I have shown that within 2 hrs following MOMP, UNDEAD cells activate NF-κB and TBK1, resulting in the release of inflammatory cytokines. My RNAseq results confirm that there is a response to IFN signaling across the myoblast

population, and overexpression of Bcl-xL has shown that the released cytokines can influence other cells by increasing their proliferation. These findings represent a novel addition to the catalogue of potential consequences of failing to undergo apoptosis.

Based on published reports that found similar results (Rongvaux et al., 2014; White et al., 2014), I presume that the activation of TBK1 and secretion of IFN-β that I have observed are dependent on post-MOMP detection of mtDNA by cGAS. I also would hypothesize that the activation of NF-κB results from activation of STING as part of the same pathway, as this has been seen in cells treated with double-stranded DNA (Abe and Barber, 2014). However, I have not directly tested this assumption. The most direct way to test it would be to deplete mtDNA so that cGAS is not activated following MOMP and see whether there was any effect on activation of either the NF-κB or IFN signaling pathways. Confirming whether cytoplasmic mtDNA is responsible for the innate immune signaling in UNDEAD cells is essential to achieving a greater understanding of these cells and the implications of their existence. Thus, mtDNA depletion experiments are currently my highest priority.

My conclusions regarding gene expression in the UNDEAD cell population are currently mostly based around the assumption that the cells in the QVD-treated clusters with abnormally low mitochondrial gene expression comprise the UNDEAD population. While later experiments did bolster this assumption by, for instance, showing that NF-κB activation occurs shortly after MOMP, thus agreeing with the expression data, the relationship between distinct subpopulations seen in the RNAseq data and those seen in imaging experiments is still uncertain. To address this, I am performing

immunofluorescence experiments that can test hypotheses derived from scRNAseq. For instance, I will see whether, as predicted, levels of proteins such as CCL2 and p62 are high in the cells with diffuse or absent cytochrome c staining.

A potential alternative explanation for the gene expression and secretion patterns I have observed is that a subpopulation of myoblasts is displaying a senescence-associated secretory phenotype (SASP). This phenotype has been characterized in a wide variety of cell types induced to senesce by a variety of stimuli and it includes the secretion of inflammatory cytokines (Coppe et al., 2010). Notably, activation of NF-κB is a hallmark of SASP (Chien et al., 2011), further suggesting it as a possible explanation for the UNDEAD phenotype. However, there are several differences between cells displaying the SASP and UNDEAD myoblasts I observe. First, at no point did any of the myoblasts treated with caspase inhibitor take on the large, flattened morphology characteristic of senescent cells. Additionally, my scRNAseq data indicate that there is hardly any expression of $p16^{INK4a}$ (*Cdkn2a*), typically upregulated in senescent cells, in any subpopulations of caspase-inhibited myoblasts. Finally, the scRNAseq data showed that the inflammatory subpopulation of myoblasts strongly upregulated cytokines, including *Ccl2* and *Ccl5*, that are not associated with the SASP. Thus, it appears unlikely that the UNDEAD cells are an inflammatory variety of senescent cells.

2.9 Materials and Methods

Cell Culture and Plasmids

C2C12 mouse myoblasts were cultured in DMEM with 10% FBS, 100 U/mL penicillin, 100 μg/mL streptomycin, and 2 mM L-Glutamine and kept in a tissue culture incubator set to 37°C and 5% CO_2. Cells were passaged every 2-3 days and were not allowed to reach more than 70% confluency. pMIG Bcl-XL and pMIG Bcl-2 were gifts from Stanley Korsmeyer (Addgene plasmid # 8790; 8793). The IMS-RP MOMP reporter construct (in pBABE) was a kind gift from Dr. Peter Sorger.

Myoblast Differentiation

C2C12 myoblasts were plated at a density of 30,000 cells/cm^2. After 24 hrs, they were washed once with PBS before the addition of differentiation media (DMEM, 2% horse serum, 100 U/mL penicillin, 100 μg/mL streptomycin and 2 mM L-Glutamine).

Plasmid Construction

pBABE-NES-DEVDG-mVenus caspase reporter

The NES-DEVDR-EYFP caspase reporter plasmid was a kind gift from Dr. Roland Eils. The portion of the plasmid coding for the cleavable peptide linker was excised by digestion with restriction endonucleases AgeI and NotI (NEB). The sense and anti-sense strands of a new linker with a mutated sequence were synthesized as oligonucleotides (IDT) with the following sequences:

Sense

5’ ccggttctagactcggaggcgtggacgaggtggacggtggcagcggc 3’

Anti-sense

5’ ggccgccgctgccaccgtccacctcgtccacgcctccgagtctagaa 3’

The oligonucleotides were mixed in equimolar quantities and annealed by slow cooling from 90°C. The 5’ ends were phosphorylated with T4 polynucleotide kinase (NEB) and the new linker was ligated into the cut plasmid. The EFYP gene was excised from the plasmid using NotI and BclI restriction enzymes and replaced using the same sites with an mVenus fluorescent reporter gene amplified with the following primers:

Forward

5’ gtgtgtgcggccgcgtgagcaagggcgaggag 3’

Reverse

5’ gtgtgttgatcagttacttgtacagctcgtccatg 3’

The entire NES-DEVDG-mVenus gene was then PCR amplified using the following primers:

Forward

5’ gtgtgtgaattctagccgccaccatgaacctgg 3’

Reverse

5’ gtgtgtgtcgacgttacttgtacagctcgtccatgc 3’

The PCR product was then ligated into the pBABE EF1α vector using EcoRI and SalI restriction sites.

pMSCV-mCherry-NLS

A 3X NLS tag was constructed by two rounds of primer annealing and extension using the following primers:

Forward 1

5’ gcatggacgagctgtacaaggatccaaaaaagaagaggaaggtagacccgaagaaaaagag 3’

Reverse 1

5’ ctctttttcttcgggtctaccttcctcttctttttttggatccttgtacagctcgtccatgc 3’

Forward 2

5’ gaagaggaaggtagacccgaagaaaaagagaaaagtcgacccaaagaagaaaaggaaagtataagcggccgcgcg 3’

Reverse 2

5’ cgcgcggccgcttatactttccttttcttctttgggtcgacttttctctttttcttcgggtctaccttcctcttc 3’

The NLS sequence was ligated into an existing construct at the 3’ end of an ER-localized mCherry gene. The mCherry-NLS portion was then PCR amplified, adding a 5’ Kozak sequence and start site, using the following primers:

Forward

5’ gtgtgtctcgaggtcgccaccatggtaagcaagggcgaggtaagtaatcc 3’

Reverse

5’ gtgtgtatcgatgtttggccgaggcggcc 3’

The PCR product was then ligated into the pLPCX vector using XhoI and ClaI restriction sites. Finally, the gene sequence was excised and cloned into a pMSCV vector with a CMV promoter using XhoI and NotI restriction sites.

pMSCV-mVenus-p65

p65 cDNA was amplified from a p65-mCherry construct (Neumann et al., 2010) using the following primers:

Forward

5’ ctctggatccgacgaactgttccccctcatc 3’

Reverse

5’ agaggcggccgcttaggagctgatctgactcag 3’

RelA cDNA was fused to mVenus by insertion into the pLPCX-Ntag-mVenus vector (a kind gift from John Albeck) using BamHI and NotI restriction sites. mVenus-p65 was PCR amplified using the following primers:

Forward

5' GAGACTCGAGGCCACCATGGTGAGCAAGGGCGAGG 3'

Reverse

5' AGAGGCGGCCGCTTAGGAGCTGATCTGACTCAG 3'

The PCR product was cloned into the pMSCV-EF1a-puro vector using XhoI and NotI restriction sites.

Cell Line Generation

Cell lines were generated using a retroviral delivery system with plasmids either in the pMSCV or pBABE vectors. HEK 293T cells at 25% confluency in a 100 mm dish were transfected with 6 μg of plasmid, 6 μg of pCL-Ampho packaging vector, and 36 μL of Fugene 6 (Promega) transfection reagent in serum free media overnight. The transfection mixture was removed and fresh DMEM was added. 48 hrs following start of transfection the media from the 293Ts was collected, sterile filtered, and concentrated 10-fold using an Amicon Ultra-15 centrifugal filter (Millipore). The concentrated virus was added to fresh DMEM with 8 μg/mL polybrene and put on C2C12 cells at 20% confluency. This process was repeated using media from the same 293Ts collected 72 hrs after transfection. After overnight

incubation with the second viral infection, C2C12s were passaged into fresh DMEM and kept for at least 2 days before start of selection with either 1.8 μg/mL puromycin or 100 μg/mL hygromycin.

Cell Sorting

C2C12 cells were harvested and washed with PBS, then resuspended in FACS buffer (PBS, 2% FBS, 1 mM EDTA) at $5x10^6$ cells/mL. Cells were sorted on a FACSAria II flow cytometer (BD Biosciences) at the Dana-Farber Cancer Institute Flow Cytometry Core Facility. Cells were re-plated in fresh DMEM media immediately after sorting.

Western Blotting

C2C12 myoblasts were washed with cold PBS and then scraped off the plate surface in the presence of lysis buffer (Tris-HCl pH6.8, 2% SDS, 10% glycerol). Lysates were passed through a 26-gauge needle to break up chromatin then centrifuged at high speed. The supernatants from each sample were boiled with β–mercaptoethanol and bromophenol blue then loaded onto a 10% polyacrylamide tris-tricine gel with equal total protein in each well. Following electrophoresis using the Mini-Protean gel electrophoresis system (Bio-Rad), proteins were transferred to a PVDF membrane using the Owl Hep-1 semidry blotting apparatus (Thermo). Membrane was blocked with Odyssey blocking buffer (LI-COR) and membranes were incubated with primary antibodies overnight at 4°C in blocking buffer. Membranes were incubated with secondary antibodies for 1 hr at RT and imaged using the Odyssey imaging system (LI-COR).

Live-Cell Microscopy

C2C12 myoblasts were seeded into wells of a 96-well imaging plate (BD 353219) 24 hrs prior to the start of imaging. The media in each well was covered with 50 uL of mineral oil to prevent evaporation. The cells were imaged on a BD Pathway 855 Bioimager using a 20x objective (0.75NA; Olympus). During imaging, the plate was kept in an environmental chamber with [CO_2] set to 5% and the temperature set such that the temperature of the media in each well was measured to be 37°C.

Immunofluorescence

Differentiated C2C12 myoblasts in 96-well imaging plates were fixed with 4% PFA and methanol. Samples were incubated with primary antibodies overnight at 4°C and with dye-conjugated secondary antibodies for 1 hr at RT in PBST with 3% BSA. DNA was stained with Hoechst dye 33342 (Cell Signaling Technology).

Antibodies

Primary antibodies for immunofluorescence: anti-myosin heavy chain (1:100, Developmental Studies Hybridoma Bank, MF-20); anti-cytochrome c (1:800, BD Pharmingen, 556432); anti-p65 (1:200, Cell Signaling Technology, 4764); anti-phospho-TBK1 (1:200, Cell Signaling Technology, 5483) For western blotting: anti-Bcl-2 (1:200, Santa Cruz, 7382); anti-Bcl-xL (1:1000, Cell Signaling Technology, 2762). Secondary antibodies for immunofluorescence: anti-mouse, anti-rabbit, and anti-goat Alexa dye conjugated (Life

Technologies). Secondary antibodies for western blotting: anti-mouse-IRDye 800 and anti-rabbit-IRDye 680 (LI-COR).

Cytokine Secretion Profiling

Supernatants were harvested from differentiating WT, Bcl-xL-OE, and Bcl-2-OE C2C12 cells 48 hrs following addition of differentiation media and treatment with either DMSO or 30 μM Q-VD-OPh. Samples were assayed using the Bio-PLex Pro Mouse Cytokine 23-Plex Assay (Bio-Rad). For each replicate for each cell line, the ratio of cytokine concentrations in the QVD-treated vs. the DMSO-treated was calculated.

Conditioned Media

C2C12 cells plated on 6-well plates were induced to differentiate by serum deprivation and treated with either DMSO, 30 μM Q-VD-OPh. Alternatively, the cells were treated with 30 μM Q-VD-OPh and 0.7 μM ABT-737 in serum free media. After 48 hrs of treatment, the media was harvested and passed through a 0.45 μm syringe filter into a Pierce Protein Concentrator PES, 3K MWCO (Thermo Scientific). Samples were spun in concentrators at 2,300 x g until volume remaining in the concentrators was 10% of the original. Volume was restored to original amount with fresh serum-free media and samples were spun for a second time. Following restoration back to the original volume and filtration using a 0.2 μm syringe filter, CM from DMSO and QVD-treated cells was diluted 2X in fresh differentiation media and then used to treat naïve C2C12s plated 24 hrs prior. CM from ABT-737 treated cells was filtered and horse serum was added to 2% before treatment of naïve C2C12s.

Functional loss of QVD activity due to dilution was assessed by observing the inability of CM to block apoptosis.

Fusion Index Calculation

Image z-stacks from a 3x3 montage of differentiated C2C12s were analyzed in Image J. Channels representing Hoechst and myosin heavy chain were merged and the myosin staining was used to manually segment the cells. Hoechst-positive nuclei were counted for every multi-nucleated cell. This value was divided by the total number of nuclei counted in the same field and then multiplied by 100 to give the fusion index.

Single-Cell RNAseq Sample Preparation

C2C12 myoblasts were plated at a density of 30,000 cells/cm^2. After 24 hrs, they were washed once with PBS and induced to differentiate via incubation with differentiation media containing either 30 μM Q-VD-OPh or DMSO. After 36 hrs of differentiation, the cells for each sample were trypsinized, counted, and then resuspended in 17% OptiPrep (Sigma) in PBS. Samples were run one at a time on the inDrop single-cell RNAseq platform as previously described (Klein et al., 2015). Briefly: flow rates through 4 inputs (cells, barcoded hydrogel beads, oil, and reverse transcription mix) were calibrated so that each droplet rarely contained more than one cell and one hydrogel bead. Emulsions were collected and reverse transcription was performed in the droplets. 1H,1H,2H,2H-Perfluorooctanol (PFO; Alfa Aesar) was added to release cDNA from droplets for library prep.

RNAseq Library Preparation

Second strand synthesis of the cDNA was done using the NEBNext® mRNA Second Strand Synthesis Module followed by *in vitro* transcription using HiScribe™ T7 High Yield RNA Synthesis Kit (New England Biolabs). The RNA was fragmented using Ambion RNA Fragmentation Reagent (Life Technologies). Reverse transcription of the RNA was done using random hexamers and a final PCR amplification was performed using Illumina indexed primers. Next generation sequencing was done using an Illumina NextSeq 500 at the Molecular Biology Core Facility at the Dana-Farber Cancer Institute.

Single-Cell RNAseq Data Analysis

Raw RNAseq data was aligned to the mouse transcriptome and processed to give an output of UMI-filtered transcript counts as previously described (Klein et al., 2015) using a python pipeline (https://github.com/indrops/indrops). Output data from the Q-VD-OPh-treated and DMSO-treated samples were analyzed both together and separately using the Seurat R toolkit (Satija et al., 2015) to do guided clustering via regression of UMI number variation, identification of highly variable genes, dimensionality reduction via principal component (PC) analysis and clustering of the most variable PCs using a smart local moving algorithm (Blondel et al., 2008) starting from a k-nearest neighbor graph. Clusters were displayed using tSNE. Gene set enrichment analysis was done using the Hallmark gene sets at the Molecular Signatures Database. Determination of gene set enrichment was done as previously described (Barbie et al., 2009).

Chapter 3: Conclusions

The two major novel findings of my dissertation research are that caspases are unlikely to be playing a non-apoptotic role in myoblast differentiation and that prevention of apoptosis can lead to the formation of UNDEAD cells that activate NF-κB in addition to the previously observed activation of type I IFN signaling. Here I will discuss the implication of this first finding on the growing literature concerned with non-apoptotic roles for caspases in various differentiation processes. I will then discuss the implications of my second finding on cellular biology in general and several diseases in particular, ending with speculation on how the presence of UNDEAD cells may affect treatment options for such diseases.

3.1 A Non-Apoptotic Role for Caspases in Differentiation?

My results have convincingly ruled out a non-apoptotic role for the apoptotic caspases in myoblast differentiation. Although my data cannot yet fully explain how conditioned media from caspase-inhibited C2C12s exerts its negative effect on differentiation, the fact that it does precludes the need for a cell-autonomous caspase activation to explain the inhibitory effect of treatment with caspase inhibitors. Indeed, the *a priori* probability that there would be another role for a protease with so many substrates whose cleavage results in disruption of normal cellular functions seems low. The data that were collected in studies looking at the differentiation of myoblasts in the context of

caspase inhibition (Fernando et al., 2002; Larsen et al., 2010; Murray et al., 2008) made a cell-autonomous role for caspases seem more likely, because at the time there was no alternative explanation for the reported observations. However, my data provide both an alternative explanation that fits with the existing evidence and new evidence that contradicts the original explanation. This now puts a heavy burden of proof on any argument that there is a non-apoptotic role for caspases in differentiating myoblasts.

This conclusion raises the question of whether some or all of the other proposed roles of apoptotic caspases in differentiation processes are incorrect. This, of course, cannot be definitively answered without additional experiments, but many of the claims are not on strong footing. First, in most cases, there is only a single publication on the topic, limiting the amount of evidence to consider. Second, the articles tend to be very reliant on population-based assays to establish caspase activation, but these cannot rule out apoptosis as the source of the observed caspase activity. Third, many studies use caspase inhibitors with fluoromethylketone (FMK) groups whose general toxicity may confound results (Chauvier et al., 2007). Finally, the observed inhibitory effects on differentiation of Bcl-2 and Bcl-xL overexpression are used to make arguments about the role of MOMP in caspase activation. However, these results could be misleading, as it has been demonstrated that effects on hematopoietic differentiation differ depending on which one of these two proteins is overexpressed (Haughn et al., 2003), suggesting a mechanism separate from their role of governing MOMP.

Nevertheless, there are some systems where a much stronger case can be made for the involvement of caspases in differentiation. Perhaps the best example is the loss of

pluripotency of ESCs (Fujita et al., 2008). In that system, a plausible substrate, Nanog, was identified that ties caspase activity to the phenotype seen upon caspase inhibition. A live-cell caspase activity reporter was also used to demonstrate a caspase-like activity in non-apoptotic cells treated with retinoic acid. That I failed to detect similar activity in differentiating myoblasts further weakens the case for caspases playing a role in the process. The last element that distinguished the ESC study from most others in the field was the use of specific caspase-3 knockout rather than reliance on chemical caspase inhibition. This sort of genetic approach allows for a more fine-tuned dissection of the role, if any, of various caspase family members. A caveat to the genetic approach is that knockout of apoptotic caspases could lead to the formation of UNDEAD cells that could influence their neighbors in a manner that would lead to the false conclusion that those caspases are providing a non-apoptotic role.

One report from the literature seems to be a particularly strong candidate to be explained by cytokine secretion from UNDEAD cells rather than non-apoptotic caspase activity. In their study, Janzen and co-authors looked at differences in the behavior of HSCs from WT or caspase-3 knockout mice. They found that caspase-3 deficiency leads to differences in downstream cell fate decisions, resulting in a relative shortage of white blood cells. They also observed increased proliferation and alterations in responsiveness of HSCs to various stimulations (Janzen et al., 2008). When taking my results into account, one can see that it is quite plausible that these effects of caspase inhibition are the result of increased pro-proliferative cytokine levels resulting from the presence of UNDEAD cells in

the vicinity of the HSCs or other cells in their lineage. Any future studies on how caspase inhibition impedes the differentiation of HSCs, or any other kind of cell, should account for this possibility when drawing conclusions.

3.2 Implications of the Rise of the UNDEAD

My discovery of UNDEAD cells within caspase-inhibited populations of myoblasts builds on the results from recent studies that discovered type I IFN signaling originating from post-MOMP, caspase-3 deficient cells (Rongvaux et al., 2014; White et al., 2014). The fate of cells that are saved from apoptosis is generally ignored, but it is now evident that, absent prompt CICD, they may become highly inflammatory, with the potential to profoundly alter the surrounding cells and tissue. Although I have yet to directly confirm whether mtDNA is the source of innate immune signaling in UNDEAD myoblasts, it seems likely. However, one question that still remains is whether mtDNA is actively being transported into the cytoplasm following MOMP, and thus is subject to regulation, or whether it passively leaks into the cytoplasm after MOMP and is thus non-regulated. Because the degree and timing of CICD is known to be variable, I believe that there is likely regulation of this response, primarily achieved by modifying the degree and timing of CICD, if not the transport of mtDNA to the cytoplasm.

To date, UNDEAD cells have only been documented in artificial systems where caspases were either knocked out or chemically inhibited. Is there evidence that UNDEAD

cells ever serve a significant biological, or physiological, function? There are a few cases that support the view that they do. Recently, Qadir and colleagues found that stimulation of the Fas death receptor in breast cancer cells increased their stem-cell-like properties via type I IFN and STAT1 signaling, and that this response was amplified when caspase-3 activity was decreased (Qadir et al., 2017). These results perfectly fit a model where death receptor stimulation triggers MOMP and then IFN signaling is activated in post-MOMP cells without sufficient caspase activation to undergo apoptosis. Ramdzan and colleagues, while making observations of AD293 cells expressing a pathological form of the huntingtin protein (Htt), discovered that cells with amyloid inclusions often avoided apoptosis and instead underwent a slow, necrotic death (Ramdzan et al., 2017). These cells may be UNDEAD cells, as they also show signs of mitochondrial depolarization. If so, this could explain the increased NF-κB target gene expression and cytokine secretion previously observed in cells with mutant Htt (Björkqvist et al., 2008). Finally, Litvin and colleagues, looking across various melanoma cell lines, concluded that high type I IFN signaling resulted in an inability to efficiently activate apoptotic caspases, even following MOMP (Litvin et al., 2015). Given what I have discovered about UNDEAD cells, I would speculate that the reverse is true and that a defect in caspase activation is causing the high IFN signaling by failing to promptly kill cells following MOMP.

That the above examples are all related to serious illnesses demonstrates the importance of better understanding the consequences of apoptotic caspase inhibition and suggests the potential for UNDEAD cells to contribute a wide variety of diseases. The most likely disease connection is to cancer, because evasion of apoptosis is one of the hallmarks

of the disease (Hanahan and Weinberg, 2000). Despite this, however, apoptotic caspases are not frequently seen as driver mutations in cancers (Olsson and Zhivotovsky, 2011). Thinking in terms of UNDEAD cells, two potential explanations for this come to mind. The first is that very few cells recover viability after undergoing MOMP, even if they avoid caspase-dependent apoptosis; thus, a loss of apoptotic caspase activity would not confer an advantage on a nascent cancer cell. The other potential explanation is that during the early stages of tumorigenesis the release of inflammatory cytokines may be detrimental to the survival of cancer cells, as they have likely not yet developed the means to avoid destruction by immune cells. In this case, loss of caspase function would be selected against via an increased chance of immune destruction. Late stage cancers, on the other hand, may be a different story. Having already adapted to avoid immune destruction, cytokine release may be less deleterious or, in fact, beneficial to them. As an example, it was recently observed that the release of Il-6 and CCL5, two cytokines secreted from UNDEAD cells, promotes growth and survival of K-Ras-driven lung cancer cells (Zhu et al., 2014). Thus, in later stage cancers, UNDEAD cells may represent a thus-far unappreciated, pro-tumorigenic element of the tumor.

If UNDEAD cells do contribute to cancer or other diseases, then there may also be potential for new therapies. As a start, being able to predict situations where UNDEAD cells are likely to be present could point to the potential importance of innate immune signaling in those instances, influencing the therapeutic approach. Learning more about CICD may also reveal ways to accelerate the death process, thus preventing UNDEAD cell formation and any deleterious effects associated with them. This approach could allow inhibition of

innate immune signaling specifically at the site of disease, thus reducing harmful side effects that could result from systemic immune inhibition. Therefore, a better understanding of UNDEAD cells and CICD has the potential to be very important for disease treatment, as well as a more thorough understanding of cellular biology, making continued work on these topics essential.

Bibliography

Abe, T., and Barber, G.N. (2014). Cytosolic-DNA-mediated, STING-dependent proinflammatory gene induction necessitates canonical NF-κB activation through TBK1. Journal of virology *88*, 5328-5341.

Albeck, J.G., Burke, J.M., Aldridge, B.B., Zhang, M., Lauffenburger, D.A., and Sorger, P.K. (2008). Quantitative Analysis of Pathways Controlling Extrinsic Apoptosis in Single Cells. Molecular cell *30*, 11-25.

Anisowicz, A., Messineo, M., Lee, S.W., and Sager, R. (1991). An NF-kappa B-like transcription factor mediates IL-1/TNF-alpha induction of gro in human fibroblasts. J Immunol *147*, 520-527.

Barbie, D.A., Tamayo, P., Boehm, J.S., Kim, S.Y., Moody, S.E., Dunn, I.F., Schinzel, A.C., Sandy, P., Meylan, E., Scholl, C.*, et al.* (2009). Systematic RNA interference reveals that oncogenic KRAS-driven cancers require TBK1. Nature *462*, 108-112.

Beaudouin, J., Liesche, C., Aschenbrenner, S., Hörner, M., and Eils, R. (2013). Caspase-8 cleaves its substrates from the plasma membrane upon CD95-induced apoptosis. Cell death and differentiation *20*, 599-610.

Bhattacharya, S., HuangFu, W.C., Dong, G., Qian, J., Baker, D.P., Karar, J., Koumenis, C., Diehl, J.A., and Fuchs, S.Y. (2013). Anti-tumorigenic effects of Type 1 interferon are subdued by integrated stress responses. Oncogene *32*, 4214-4221.

Bischoff, R., and Holtzer, H. (1969). Mitosis and the processes of differentiation of myogenic cells in vitro. J Cell Biol *41*, 188-200.

Björkqvist, M., Wild, E.J., Thiele, J., Silvestroni, A., Andre, R., Lahiri, N., Raibon, E., Lee, R.V., Benn, C.L., Soulet, D.*, et al.* (2008). A novel pathogenic pathway of immune activation detectable before clinical onset in Huntington's disease. The Journal of experimental medicine *205*, 1869-1877.

Blasche, S., Mörtl, M., Steuber, H., Siszler, G., Nisa, S., Schwarz, F., Lavrik, I., Gronewold, T.M.A., Maskos, K., Donnenberg, M.S.*, et al.* (2013). The E. coli effector protein NleF is a caspase inhibitor. PloS one *8*, e58937.

Blondel, V.D., Guillaume, J.-L., Lambiotte, R., and Lefebvre, E. (2008). Fast unfolding of communities in large networks. Journal of Statistical Mechanics: Theory and Experiment *2008*, P10008.

Callus, B.A., and Vaux, D.L. (2007). Caspase inhibitors: viral, cellular and chemical. Cell death and differentiation *14*, 73-78.

Carlile, G.W., Smith, D.H., and Wiedmann, M. (2004). Caspase-3 has a nonapoptotic function in erythroid maturation. Blood *103*, 4310-4316.

Casar, J.C., McKechnie, B.A., Fallon, J.R., Young, M.F., and Brandan, E. (2004). Transient up-regulation of biglycan during skeletal muscle regeneration: delayed fiber growth along with decorin increase in biglycan-deficient mice. Developmental biology *268*, 358-371.

Chauvier, D., Ankri, S., Charriaut-Marlangue, C., Casimir, R., and Jacotot, E. (2007). Broad-spectrum caspase inhibitors: from myth to reality? Cell Death Differ *14*, 387-391.

Cheng, E.H., Wei, M.C., Weiler, S., Flavell, R.A., Mak, T.W., Lindsten, T., and Korsmeyer, S.J. (2001). BCL-2, BCL-X(L) sequester BH3 domain-only molecules preventing BAX- and BAK-mediated mitochondrial apoptosis. Molecular cell *8*, 705-711.

Chien, Y., Scuoppo, C., Wang, X., Fang, X., Balgley, B., Bolden, J.E., Premsrirut, P., Luo, W., Chicas, A., Lee, C.S.*, et al.* (2011). Control of the senescence-associated secretory phenotype by NF-kappaB promotes senescence and enhances chemosensitivity. Genes Dev *25*, 2125-2136.

Colell, A., Ricci, J.-E., Tait, S., Milasta, S., Maurer, U., Bouchier-Hayes, L., Fitzgerald, P., Guio-Carrion, A., Waterhouse, N.J., Li, C.W.*, et al.* (2007). GAPDH and autophagy preserve survival after apoptotic cytochrome c release in the absence of caspase activation. Cell *129*, 983-997.

Coppe, J.P., Desprez, P.Y., Krtolica, A., and Campisi, J. (2010). The senescence-associated secretory phenotype: the dark side of tumor suppression. Annu Rev Pathol *5*, 99-118.

Cosentino, K., and García-Sáez, A.J. (2017). Bax and Bak Pores: Are We Closing the Circle? Trends in cell biology *27*, 266-275.

Danial, N.N., Gramm, C.F., Scorrano, L., Zhang, C.-Y., Krauss, S., Ranger, A.M., Datta, S.R., Greenberg, M.E., Licklider, L.J., Lowell, B.B.*, et al.* (2003). BAD and glucokinase reside in a mitochondrial complex that integrates glycolysis and apoptosis. Nature *424*, 952-956.

De Botton, S., Sabri, S., Daugas, E., Zermati, Y., Guidotti, J.E., Hermine, O., Kroemer, G., Vainchenker, W., and Debili, N. (2002). Platelet formation is the consequence of caspase activation within megakaryocytes. Blood *100*, 1310-1317.

DeBartolo, J., Dutta, S., Reich, L., and Keating, A.E. (2012). Predictive Bcl-2 family binding models rooted in experiment or structure. J Mol Biol *422*, 124-144.

Degterev, A., Huang, Z., Boyce, M., Li, Y., Jagtap, P., Mizushima, N., Cuny, G.D., Mitchison, T.J., Moskowitz, M.A., and Yuan, J. (2005). Chemical inhibitor of nonapoptotic cell death with therapeutic potential for ischemic brain injury. Nature chemical biology *1*, 112-119.

Dick, S.A., Chang, N.C., Dumont, N.A., Bell, R.A.V., Putinski, C., Kawabe, Y., Litchfield, D.W., Rudnicki, M.A., and Megeney, L.A. (2015). Caspase 3 cleavage of Pax7 inhibits self-renewal of satellite cells. Proceedings of the National Academy of Sciences of the United States of America *112*, E5246-5252.

Epting, C.L., López, J.E., Shen, X., Liu, L., Bristow, J., and Bernstein, H.S. (2004). Stem cell antigen-1 is necessary for cell-cycle withdrawal and myoblast differentiation in C2C12 cells. Journal of cell science *117*, 6185-6195.

Feltham, R., Vince, J.E., and Lawlor, K.E. (2017). Caspase-8: not so silently deadly. Clinical & translational immunology *6*, e124.

Fernando, P., Kelly, J.F., Balazsi, K., Slack, R.S., and Megeney, L.A. (2002). Caspase 3 activity is required for skeletal muscle differentiation. Proceedings of the National Academy of Sciences of the United States of America *99*, 11025-11030.

Foley, J.D., Rosenbaum, H., and Griep, A.E. (2004). Temporal regulation of VEID-7-amino-4-trifluoromethylcoumarin cleavage activity and caspase-6 correlates with organelle loss during lens development. J Biol Chem *279*, 32142-32150.

Fujita, J., Crane, A.M., Souza, M.K., Dejosez, M., Kyba, M., Flavell, R.A., Thomson, J.A., and Zwaka, T.P. (2008). Caspase activity mediates the differentiation of embryonic stem cells. Cell stem cell *2*, 595-601.

Gamble, H.J., Fenton, J., and Allsopp, G. (1978). Electron microscope observations on human fetal striated muscle. J Anat *126*, 567-589.

Guicciardi, M.E., and Gores, G.J. (2009). Life and death by death receptors. FASEB J *23*, 1625-1637.

Hanahan, D., and Weinberg, R.A. (2000). The hallmarks of cancer. Cell *100*, 57-70.

Haskill, S., Beg, A.A., Tompkins, S.M., Morris, J.S., Yurochko, A.D., Sampson-Johannes, A., Mondal, K., Ralph, P., and Baldwin, A.S., Jr. (1991). Characterization of an immediate-early gene induced in adherent monocytes that encodes I kappa B-like activity. Cell *65*, 1281-1289.

Haughn, L., Hawley, R.G., Morrison, D.K., von Boehmer, H., and Hockenbery, D.M. (2003). BCL-2 and BCL-XL restrict lineage choice during hematopoietic differentiation. The Journal of biological chemistry *278*, 25158-25165.

Hengartner, M.O. (2000). The biochemistry of apoptosis. Nature *407*, 770-776.

Hill, M.M., Adrain, C., Duriez, P.J., Creagh, E.M., and Martin, S.J. (2004). Analysis of the composition, assembly kinetics and activity of native Apaf-1 apoptosomes. EMBO J *23*, 2134-2145.

Hoesel, B., and Schmid, J.A. (2013). The complexity of NF-kappaB signaling in inflammation and cancer. Mol Cancer *12*, 86.

Hung, Y.P., Albeck, J.G., Tantama, M., and Yellen, G. (2011). Imaging cytosolic NADH-NAD(+) redox state with a genetically encoded fluorescent biosensor. Cell Metab *14*, 545-554.

Ichim, G., Lopez, J., Ahmed, S.U., Muthalagu, N., Giampazolias, E., Delgado, M.E., Haller, M., Riley, J.S., Mason, S.M., Athineos, D*., et al.* (2015). Limited mitochondrial permeabilization causes DNA damage and genomic instability in the absence of cell death. Molecular cell *57*, 860-872.

Ishizaki, Y., Jacobson, M.D., and Raff, M.C. (1998). A role for caspases in lens fiber differentiation. The Journal of cell biology *140*, 153-158.

Janzen, V., Fleming, H.E., Riedt, T., Karlsson, G., Riese, M.J., Lo Celso, C., Reynolds, G., Milne, C.D., Paige, C.J., Karlsson, S.*, et al.* (2008). Hematopoietic stem cell responsiveness to exogenous signals is limited by caspase-3. Cell stem cell *2*, 584-594.

Johnson, D.E., Ai, H.W., Wong, P., Young, J.D., Campbell, R.E., and Casey, J.R. (2009). Red fluorescent protein pH biosensor to detect concentrative nucleoside transport. J Biol Chem *284*, 20499-20511.

Karin, M. (1999). How NF-kappaB is activated: the role of the IkappaB kinase (IKK) complex. Oncogene *18*, 6867-6874.

Klein, A.M., Mazutis, L., Akartuna, I., Tallapragada, N., Veres, A., Li, V., Peshkin, L., Weitz, D.A., and Kirschner, M.W. (2015). Droplet barcoding for single-cell transcriptomics applied to embryonic stem cells. Cell *161*, 1187-1201.

Krauss, S.W., Lo, A.J., Short, S.A., Koury, M.J., Mohandas, N., and Chasis, J.A. (2005). Nuclear substructure reorganization during late-stage erythropoiesis is selective and does not involve caspase cleavage of major nuclear substructural proteins. Blood *106*, 2200-2205.

Kroemer, G., Galluzzi, L., and Brenner, C. (2007). Mitochondrial membrane permeabilization in cell death. Physiological reviews *87*, 99-163.

Krumschnabel, G., Sohm, B., Bock, F., Manzl, C., and Villunger, A. (2009). The enigma of caspase-2: the laymen's view. Cell death and differentiation *16*, 195-207.

Larsen, B.D., Rampalli, S., Burns, L.E., Brunette, S., Dilworth, F.J., and Megeney, L.A. (2010). Caspase 3/caspase-activated DNase promote cell differentiation by inducing DNA strand breaks. Proceedings of the National Academy of Sciences of the United States of America *107*, 4230-4235.

Li, H., Zhu, H., Xu, C.J., and Yuan, J. (1998a). Cleavage of BID by caspase 8 mediates the mitochondrial damage in the Fas pathway of apoptosis. Cell *94*, 491-501.

Li, X., Zhao, X., Fang, Y., Jiang, X., Duong, T., Fan, C., Huang, C.C., and Kain, S.R. (1998b). Generation of destabilized green fluorescent protein as a transcription reporter. J Biol Chem *273*, 34970-34975.

Libermann, T.A., and Baltimore, D. (1990). Activation of interleukin-6 gene expression through the NF-kappa B transcription factor. Mol Cell Biol *10*, 2327-2334.

Litvin, O., Schwartz, S., Wan, Z., Schild, T., Rocco, M., Oh, N.L., Chen, B.-J., Goddard, N., Pratilas, C., and Pe'er, D. (2015). Interferon α/β Enhances the Cytotoxic Response of MEK Inhibition in Melanoma. Molecular cell *57*, 784-796.

Molkentin, J.D., and Olson, E.N. (1996). Combinatorial control of muscle development by basic helix-loop-helix and MADS-box transcription factors. Proc Natl Acad Sci U S A *93*, 9366-9373.

Murray, T.V.A., McMahon, J.M., Howley, B.A., Stanley, A., Ritter, T., Mohr, A., Zwacka, R., and Fearnhead, H.O. (2008). A non-apoptotic role for caspase-9 in muscle differentiation. Journal of cell science *121*, 3786-3793.

Nakano, K., and Vousden, K.H. (2001). PUMA, a novel proapoptotic gene, is induced by p53. Mol Cell *7*, 683-694.

Neumann, L., Pforr, C., Beaudouin, J., Pappa, A., Fricker, N., Krammer, P.H., Lavrik, I.N., and Eils, R. (2010). Dynamics within the CD95 death-inducing signaling complex decide life and death of cells. Molecular systems biology *6*, 352.

Oh, J., Sinha, I., Tan, K.Y., Rosner, B., Dreyfuss, J.M., Gjata, O., Tran, P., Shoelson, S.E., and Wagers, A.J. (2016). Age-associated NF-κB signaling in myofibers alters the satellite cell niche and re-strains muscle stem cell function. Aging *8*, 2871-2896.

Olsson, M., and Zhivotovsky, B. (2011). Caspases and cancer. Cell death and differentiation *18*, 1441-1449.

Pelengaris, S., and Khan, M. (2013). The Molecular Biology of Cancer (John Wiley & Sons).

Poreba, M., Szalek, A., Rut, W., Kasperkiewicz, P., Rutkowska-Wlodarczyk, I., Snipas, S.J., Itoh, Y., Turk, D., Turk, B., Overall, C.M*., et al.* (2017). Highly sensitive and adaptable fluorescence-quenched pair discloses the substrate specificity profiles in diverse protease families. Scientific reports *7*, 43135.

Qadir, A.S., Ceppi, P., Brockway, S., Law, C., Mu, L., Khodarev, N.N., Kim, J., Zhao, J.C., Putzbach, W., Murmann, A.E.*, et al.* (2017). CD95/Fas Increases Stemness in Cancer Cells by Inducing a STAT1-Dependent Type I Interferon Response. Cell reports *18*, 2373-2386.

Ramdzan, Y.M., Trubetskov, M.M., Ormsby, A.R., Newcombe, E.A., Sui, X., Tobin, M.J., Bongiovanni, M.N., Gras, S.L., Dewson, G., Miller, J.M.L.*, et al.* (2017). Huntingtin Inclusions Trigger Cellular Quiescence, Deactivate Apoptosis, and Lead to Delayed Necrosis. Cell reports *19*, 919-927.

Rongvaux, A., Jackson, R., Harman, C.C.D., Li, T., West, A.P., de Zoete, M.R., Wu, Y., Yordy, B., Lakhani, S.A., Kuan, C.-Y.*, et al.* (2014). Apoptotic caspases prevent the induction of type I interferons by mitochondrial DNA. Cell *159*, 1563-1577.

Salmena, L., Lemmers, B., Hakem, A., Matysiak-Zablocki, E., Murakami, K., Au, P.Y., Berry, D.M., Tamblyn, L., Shehabeldin, A., Migon, E.*, et al.* (2003). Essential role for caspase 8 in T-cell homeostasis and T-cell-mediated immunity. Genes Dev *17*, 883-895.

Satija, R., Farrell, J.A., Gennert, D., Schier, A.F., and Regev, A. (2015). Spatial reconstruction of single-cell gene expression data. Nature biotechnology *33*, 495-502.

Sordet, O., Rébé, C., Plenchette, S., Zermati, Y., Hermine, O., Vainchenker, W., Garrido, C., Solary, E., and Dubrez-Daloz, L. (2002). Specific involvement of caspases in the differentiation of monocytes into macrophages. Blood *100*, 4446-4453.

Stennicke, H.R., Renatus, M., Meldal, M., and Salvesen, G.S. (2000). Internally quenched fluorescent peptide substrates disclose the subsite preferences of human caspases 1, 3, 6, 7 and 8. Biochem J *350 Pt 2*, 563-568.

Tait, S.W., and Green, D.R. (2013). Mitochondrial regulation of cell death. Cold Spring Harb Perspect Biol *5*.

Tait, S.W.G., Parsons, M.J., Llambi, F., Bouchier-Hayes, L., Connell, S., Muñoz-Pinedo, C., and Green, D.R. (2010). Resistance to caspase-independent cell death requires persistence of intact mitochondria. Developmental cell *18*, 802-813.

Tanaka, K., Sato, K., Yoshida, T., Fukuda, T., Hanamura, K., Kojima, N., Shirao, T., Yanagawa, T., and Watanabe, H. (2011). Evidence for cell density affecting C2C12 myogenesis: possible regulation of myogenesis by cell-cell communication. Muscle Nerve *44*, 968-977.

Taylor, R.C., Cullen, S.P., and Martin, S.J. (2008). Apoptosis: controlled demolition at the cellular level. Nat Rev Mol Cell Biol *9*, 231-241.

Ueda, A., Okuda, K., Ohno, S., Shirai, A., Igarashi, T., Matsunaga, K., Fukushima, J., Kawamoto, S., Ishigatsubo, Y., and Okubo, T. (1994). NF-kappa B and Sp1 regulate transcription of the human monocyte chemoattractant protein-1 gene. J Immunol *153*, 2052-2063.

van Pesch, V., Lanaya, H., Renauld, J.C., and Michiels, T. (2004). Characterization of the murine alpha interferon gene family. J Virol *78*, 8219-8228.

Walczak, H. (2013). Death receptor-ligand systems in cancer, cell death, and inflammation. Cold Spring Harb Perspect Biol *5*, a008698.

White, M.J., McArthur, K., Metcalf, D., Lane, R.M., Cambier, J.C., Herold, M.J., van Delft, M.F., Bedoui, S., Lessene, G., Ritchie, M.E.*, et al.* (2014). Apoptotic caspases suppress mtDNA-induced STING-mediated type I IFN production. Cell *159*, 1549-1562.

Wride, M.A., Parker, E., and Sanders, E.J. (1999). Members of the bcl-2 and caspase families regulate nuclear degeneration during chick lens fibre differentiation. Developmental biology *213*, 142-156.

Xu, X., Gerard, A.L., Huang, B.C., Anderson, D.C., Payan, D.G., and Luo, Y. (1998). Detection of programmed cell death using fluorescence energy transfer. Nucleic Acids Res *26*, 2034-2035.

Yaffe, D., and Saxel, O. (1977). Serial passaging and differentiation of myogenic cells isolated from dystrophic mouse muscle. Nature *270*, 725-727.

Yahiaoui, L., Gvozdic, D., Danialou, G., Mack, M., and Petrof, B.J. (2008). CC family chemokines directly regulate myoblast responses to skeletal muscle injury. The Journal of physiology *586*, 3991-4004.

Yip, K.W., and Reed, J.C. (2008). Bcl-2 family proteins and cancer. Oncogene *27*, 6398-6406.

Yuan, S., Yu, X., Asara, J.M., Heuser, J.E., Ludtke, S.J., and Akey, C.W. (2011). The holo-apoptosome: activation of procaspase-9 and interactions with caspase-3. Structure *19*, 1084-1096.

Zandy, A.J., Lakhani, S., Zheng, T., Flavell, R.A., and Bassnett, S. (2005). Role of the executioner caspases during lens development. The Journal of biological chemistry *280*, 30263-30272.

Zermati, Y., Garrido, C., Amsellem, S., Fishelson, S., Bouscary, D., Valensi, F., Varet, B., Solary, E., and Hermine, O. (2001). Caspase activation is required for terminal erythroid differentiation. The Journal of experimental medicine *193*, 247-254.

Zhai, D., Yu, E., Jin, C., Welsh, K., Shiau, C.-w., Chen, L., Salvesen, G.S., Liddington, R., and Reed, J.C. (2010). Vaccinia virus protein F1L is a caspase-9 inhibitor. The Journal of biological chemistry *285*, 5569-5580.

Zhu, Z., Aref, A.R., Cohoon, T.J., Barbie, T.U., Imamura, Y., Yang, S., Moody, S.E., Shen, R.R., Schinzel, A.C., Thai, T.C*., et al.* (2014). Inhibition of KRAS-driven tumorigenicity by interruption of an autocrine cytokine circuit. Cancer discovery *4*, 452-465.